BMC Genomics

RESEARCH

Open Access

Exploring *Pinus nigra's* induced defense arsenal against *Diplodia sapinea* through gene and metabolic pathway analysis

Carlos Trujillo-Moya[1*†], Sanna Olsson[2†], Susanne Mottinger-Kroupa[3], Erhard Halmschlager[3], Reinhard Ertl[4], Oliver Gailing[5], Barbara Vornam[5^], Bruno Fady[6], Andrea Ganthaler[7], Muhammad Ahmad[1], Ana Espinosa-Ruiz[8], Esther Carrera[8], Maria Ángeles Martínez-Godoy[8], Jorge Baños[8], Clara Priemer[9], Jan-Peter George[10] and Marcela van Loo[1]

Abstract

The European black pine (*Pinus nigra* J. F. Arnold) is a conifer of high economic and ecological importance and is considered a potential alternative to several forest tree species in Central Europe to support adaptation to global climate warming. However, the fungus *Diplodia sapinea* (Fr.) Fuckel is causing severe damage and world-wide economic loss to this and other Pinus host species. The lack of genomic resources and the scarce knowledge of the tree´s molecular defense mechanisms limit any breeding perspectives. Here, we report the results of a controlled infection experiment in which the transcriptomic and metabolomic profiles of mock and infected *P. nigra* saplings from two provenances were compared over a period of 21 days. This combined approach suggests that *P. nigra* response to *D. sapinea* infection is activated between 8 and 21 days post-inoculation when key plant defense signaling hormones such as jasmonic acid, abscisic acid and salicylic acid increased. This concurred with high differential gene expression, including the activation of major plant defense-related pathways, leading to the induction of several phytoalexins and defense-related proteins. Furthermore, some of these responses were provenance-specific. Finally, this study identified key genes and metabolic pathways involved in the defense response of *P. nigra* to *D. sapinea*, providing a solid basis for further exploration of genetic variation among natural populations (provenances) of different subspecies with varying constitutive and induced defense responses. This deeper understanding will aid in elucidating resistance mechanisms and guiding the selection of plant reproductive material for future forest plantations.

Keywords Conifers, Black pine, *Diplodia* tip blight, Transcriptomics, Metabolomics, Plant defense response, Plant hormones, Phenolics, Terpenoids, Plant-pathogen interaction

[†]Carlos Trujillo-Moya and Sanna Olsson contributed equally and should be both consider as first authors.

[^]Barbara Vornam is deceased. This paper is dedicated to her memory.

*Correspondence:
Carlos Trujillo-Moya
carlos.trujillo-moya@bfw.gv.at

Full list of author information is available at the end of the article

Introduction

Climate change markedly modifies forest disturbance regimes on a global scale [1] by increasing pathogen-related disruptions [2, 3], leading to severe economic loss [4] and ecological challenges [5]. Consequently, studies on tree-pathogen interactions and studies deciphering the basis of forest tree adaptation and resilience to pathogens have intensified in recent years [6–11].

The European black pine (*Pinus nigra* J. F. Arnold) is a peri-Mediterranean conifer tree species with high economic and ecological importance that is found across Europe, Asia Minor, and North Africa in a wide range of habitats. In addition to timber production, it is also used in reforestation programs to effectively control soil erosion and landslides, as well as for land rehabilitation [5, 12]. *P. nigra* is genetically and phenotypically variable, with several loosely differentiated subspecies that easily interbreed [13–15]. In this study, we consider two ecologically divergent provenances, an Austrian provenance (*P. nigra* subsp. *nigra*) originating from Central European continental climates with colder winters and relatively regular precipitation, and a Corsican provenance (*P. nigra* subsp. *laricio*) adapted to Mediterranean mountain environments characterized by warmer temperatures and pronounced summer drought. It has been proposed as one of the most promising tree species for assisted migration in Central Europe [16] under many climate change scenarios due to its higher tolerance to drought compared to other coniferous species [5, 17]. However, the species is severely affected by a fungal disease caused by the widespread ascomycete *Diplodia sapinea* (Fr.) Fuckel (syn. *Diplodia pinea* (Desm.) Kickx., *Sphaeropsis sapinea* (Fr.: Fr.) Dyko and Sutton) [18, 19]. The fungus is an opportunistic, and necrotrophic pathogen of conifers causing worldwide economic losses [20–22].

Horizontal transmission of *D. sapinea* among nearby living trees is the primary mode of infection [23], as the fungus can enter plants through small wounds and can invade tissues, and may also cause shoot blight, crown dieback, blue staining of wood, bark necrosis, and ultimately tree death [24, 25]. However, vertical transmission from the mother tree to offspring can occur, resulting in a high risk for seeds to become colonized by the pathogen [23], further contributing to the dissemination of *D. sapinea* and making it one of the most widespread conifer pathogens in the world (CABI Invasive Species Compendium: http://www.cabi.org/isc/datasheet/19160). This endophytic fungus may also cause latent infections with long periods of dormancy in apparently healthy trees [26, 27] until stressful environmental conditions such as drought or hail weaken the host and trigger its pathogenicity [28, 29]. Latent infections of *D. sapinea* can be detected in asymptomatic tissue [28, 30, 31] only by molecular biological methods [23, 32–35]. While selection of resistant or less susceptible material of this species can be highly promising for effective disease management [36], there is still limited understanding of the interactions between pine hosts and *D. sapinea*, as noted by [37].

In *P. nigra*, *D. sapinea* is known to induce various defense responses, both locally at infection sites and systemically in distant tissues, enhancing whole-plant resistance to subsequent biotic stress through systemic induced resistance (SIR) [38–40]. Nevertheless, the induced response can be dependent on the site of infection (i.e., lower stem, upper stem, shoots) [41, 42], resulting in either SIR or systemic induced susceptibility (SIS) when defenses of symptomatic trees are weaker against future attacks. In addition, drought-derived perturbations can contribute to enhanced susceptibility [43, 44]. The analysis of phytohormones, phenolic compounds, and terpenoids involved in pathogen-induced defense mechanisms is important from a metabolic perspective, as these compounds act either as signaling and regulatory molecules or as direct inhibitors of pathogen activity. For instance, in Scots pine (*P. sylvestris*) infected by *D. sapinea*, plant hormones such as jasmonic acid (JA), abscisic acid (ABA), salicylic acid (SA) and others lead to the induction of defensive chemicals (phytoalexins), proteins and anatomical defenses [37, 45, 46]. Similarly, SIR in *P. nigra* stems is associated with induced lignification [41, 47] and accumulation of flavonoids such as taxifolin [48], supporting a potential role of these and other phytoalexins such as phenolic glycosides and stilbenes [49, 50] in disease resistance. However, tree resistance cannot be predicted from phenolic profiles alone, as their significant accumulation in symptomatic trees may also be indicative of other stress factors, rather than a defense response to fungal infection [42, 51]. Terpenoids are another major class of specialized metabolites in pines, and while they have not been consistently associated with SIR in this pathosystem so far [49, 52] as they have been for *Pinus pinea* L. [53], they are generally considered antimicrobial [54] and could at least partly contribute to reductions in stem lesion length [42].

The genetic dissection of the systemic induced defense response can help to effectively combat this pathogen in the near future. However, genetic studies remain challenging for conifer species due to the limited knowledge of genetic variation in natural populations, polygenic inheritance of several traits, and difficulties to do accurate phenotypic prediction assessments [34]. Transcriptomics is a powerful tool to reduce the genomic complexity of fully sequenced conifer genomes, targeting specific genes [8, 55–57], and complementing association studies [58]. Due to the limited availability of reference genomes for most conifer species, which is primarily attributed to their exceptionally large genomes

rich in repetitive sequences and pseudogenes [59], current research predominantly relies on transcriptome data. Transcriptome resources are now available for an increasing number of pine species and have been used for several applications including RNA-seq, a standard tool for investigating genome-wide differential gene expression under contrasting abiotic [60] and biotic stresses [6, 9, 61]. For instance, defense transcriptomics of Scots pine saplings artificially infected with *D. sapinea* revealed the induction of genes involved in lignin- and phytoalexin-biosynthesis and pathogenesis-related genes that can serve as targets for resistance breeding [62]. Recently, [44] integrated concurrent host and pathogen responses in *P. nigra* based on simultaneous transcriptomic analyses at early stages of the infection (≤ 72 h), while late molecular responses remain uncharted.

In the present study, we investigated, for the first time, the molecular responses of two *P. nigra* provenances (Austrian and Corsican) representing two different subspecies with distinct ecological backgrounds to a *D. sapinea* infection (single exposure). We used a combined transcriptomic (RT-qPCR, RNA-seq) and metabolomic (phytohormones, phenolic compounds, diterpenes and volatile organic compounds (VOCs) approach in a greenhouse-controlled infection experiment for a period of 21 days (Figure S1). The timeframe studied here was selected based on the existing literature and on standard practices when dissecting a pathosystem molecularly. RT-qPCR was used to identify the time point with the most notable differential expression for further in-depth analysis by mRNA sequencing. Due to the lack of a *P. nigra* reference genome, we explored the most reasonable alternatives for establishing a suitable standard RNA-seq protocol. First, we used the only publicly available reference transcriptome of *P. nigra*, generated to study genetic lineages and based on adult needle tissue [63]. Second, the comprehensive reference transcriptome of a closely related pine species, *P. sylvestris*, was used, which combines different tissue types and developmental stages [64]. Finally, with the main aim to identify genes and metabolic pathways involved in the induced defense response, we hypothesised that: (i) stem inoculation of two-year-old *P. nigra* saplings with *D. sapinea* would trigger systemic induced reactions in the terminal shoot needles, including shared and provenance-specific reactions; (ii) these responses would include significant alternations in stress-related phytohormone profiles, which activate plant defense signalling pathways; and (iii) subsequent differential gene expression would coincide with significant changes in defense proteins and concentrations of plant secondary metabolites, such as phenolic and terpenoid compounds.

Results

RT-qPCR on candidate defense-related genes

After 21 days, all *D. sapinea* inoculated (further referred to as inoculated or infected) saplings of the two different provenances (Austrian, Corsican) showed clear symptoms of infection, while mock inoculated (further referred to as mock) plants showed no symptoms throughout the entire infection experiment. The expression stability of the four candidate reference genes (RGs) α-Tubulin, Actin (ACT), α-Tubulin (ATUB), and Ubiquitine (UBI) were evaluated in the needles. ACT and ATUB were identified as the two most stably expressed genes and were selected for normalization (Figure S2). Most of the twenty-one *P. nigra* candidate defense related orthologs selected for RT-qPCR analysis for all time points (for more details see Materials & Methods) showed a notable induced expression occurring in 21 days post-inoculation (dpi) samples (Figure S3) for both the Corsican (19 genes) and the Austrian (12 genes) provenance. The highest levels of up-regulation at 21 dpi were found in Corsican plants for the *P. sylvestris* orthologs Glucan endo-1,3-beta-glucosidase (contig_28064), endochitinase CH5B (contig_48603), and the *Picea abies* (L.) H. Karst ortholog basic endochitinase B (contig_26700).

A principal component analysis (PCA), using delta Cq values of all transcripts, grouped all mock and 3—8 dpi inoculated samples due to their high similarity in their expression profiles (Fig. 1). However, at 21 dpi, infected plants were segregated for Austrian and Corsican provenances. Additionally, 21 dpi (PC1: 80.1% explained variance) appeared to be the most significant time point for divergence, further explored via mRNA sequencing and differential gene expression analysis.

21 dpi cDNA sequencing (mRNA-seq) and mapping to the available reference transcriptomes with different alignment methods

All samples from 21 dpi were used for mRNA-seq, from which a total of 14.61 million single-end reads were obtained via cDNA sequencing (Illumina NextSeq 500; Illumina, San Diego, CA, USA) of the libraries (QuantSeq 3' mRNA-seq FWD) generated from needles. The number of input reads after quality control trimming varied between 9.8 million and 16.28 million depending on treatment and provenance (Table S1), with an average input read length of 71 base pairs. Sequence alignment (BWA-MEM) to the *D. sapinea* reference genome was then performed, and the fungus was detected in all samples. The number of reads that uniquely aligned to *D. sapinea* varied between 0.37 million and 1.19 million (3.04% to 9.45% of the total reads; 4.85% on average), except for one of the infected Corsican samples in which 5.65 million reads aligned to the fungal genome (40.41% of the total reads).

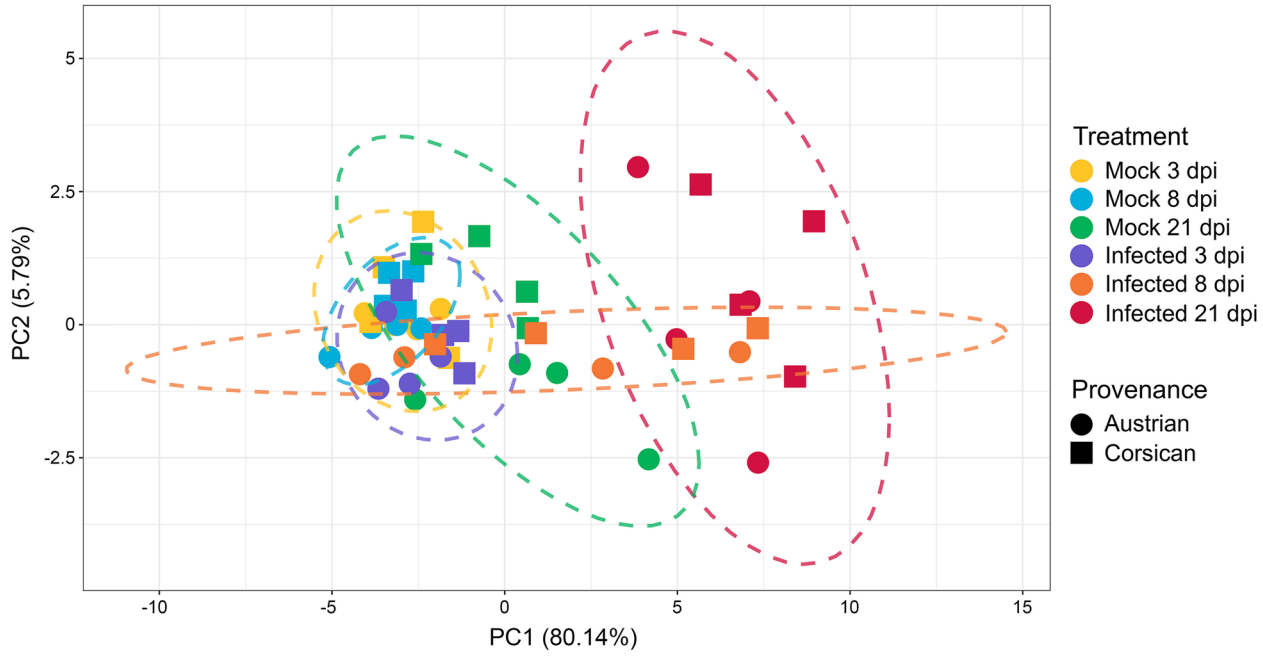

Fig. 1 Principal component analysis (PCA) plot derived from delta Cq values (RT-qPCR) of 21 candidate defense related transcripts, performed on needle samples from mock and inoculated saplings for time points 3, 8, and 21 dpi. The dashed circles indicate the 95% confidence intervals for each experimental group. Note the distinct separation of most 8 dpi and all 21 dpi inoculated samples from mock for both Austrian and Corsican sample replicates

Once *D. sapinea* reads were filtered out, the number of remaining input reads varied between 8.33 million and 15.45 million depending on treatment and provenance. When the alignment method BWA-MEM was used, the number of reads that uniquely aligned to the *P. nigra* reference transcriptome varied between 4.43 million and 7.6 million (51% of the total reads on average), while the mapped reads were reduced to 3.75—6.54 million (44% of the total reads on average) when the Salmon alignment method was applied. A similar outcome was observed when the *P. sylvestris* reference transcriptome was employed, although resulting in higher alignment rates. The number of reads uniquely aligning to *P. sylvestris* ranged from 5.77 million to 13.25 million, accounting for an average of 84% of the total reads, when utilizing BWA-MEM. On the other hand, the use of Salmon reduced the alignment rate to 67% on average. In all cases, the inter-replicate correlation between the biological replicates for each treatment and provenance combination was high (R^2: 0.901 ± 0.04), suggesting that the cDNA sequencing yielded reliable data for downstream analyses.

Differential gene expression patterns between treatments and provenances

The PCA of the overall differential gene expression profile confirmed the large differences between mock and inoculated trees at 21 dpi (Fig. 2), also observed during candidate genes´ RT-qPCR. This pattern, reflected by component 1 (62–78% variance), was observed for both provenances (Austrian and Corsican) regardless of the reference transcriptome (*P. nigra* or *P. sylvestris*) and alignment method used (BWA-MEM or Salmon). The distance between mock samples from the same provenance was greater for the Austrian samples than for the Corsican ones when *P. sylvestris* was used as the reference instead of *P. nigra.* Nevertheless, differences between samples reflected along PC2 were minor (6–7% variance).

Global analysis of differentially expressed genes (DEGs)

Regardless of the alignment method and reference transcriptome selected, an average of 5206 transcripts were differentially expressed in the needles of inoculated samples when compared to those of mock samples, with a slight tendency towards down-regulation (42% up- compared to 58% down-regulated DEGs) (Fig. 3 and Table S2). A set of 778 up- and 1622 down-regulated DEGs were shared between all provenances and alignment methods (termed CONSERVATIVE) when *P. nigra* was considered as reference transcriptome, while 534 up- and 957 down-regulated DEGs were identified using *P. sylvestris*. When considering DEGs shared by both provenances in at least one alignment method (termed RELAXED), the number of shared genes increased to 1056 up- and 2003 down-regulated DEGs with *P. nigra* as the reference, or 1846 up- and 2894 down-regulated DEGs when using *P. sylvestris* as reference.

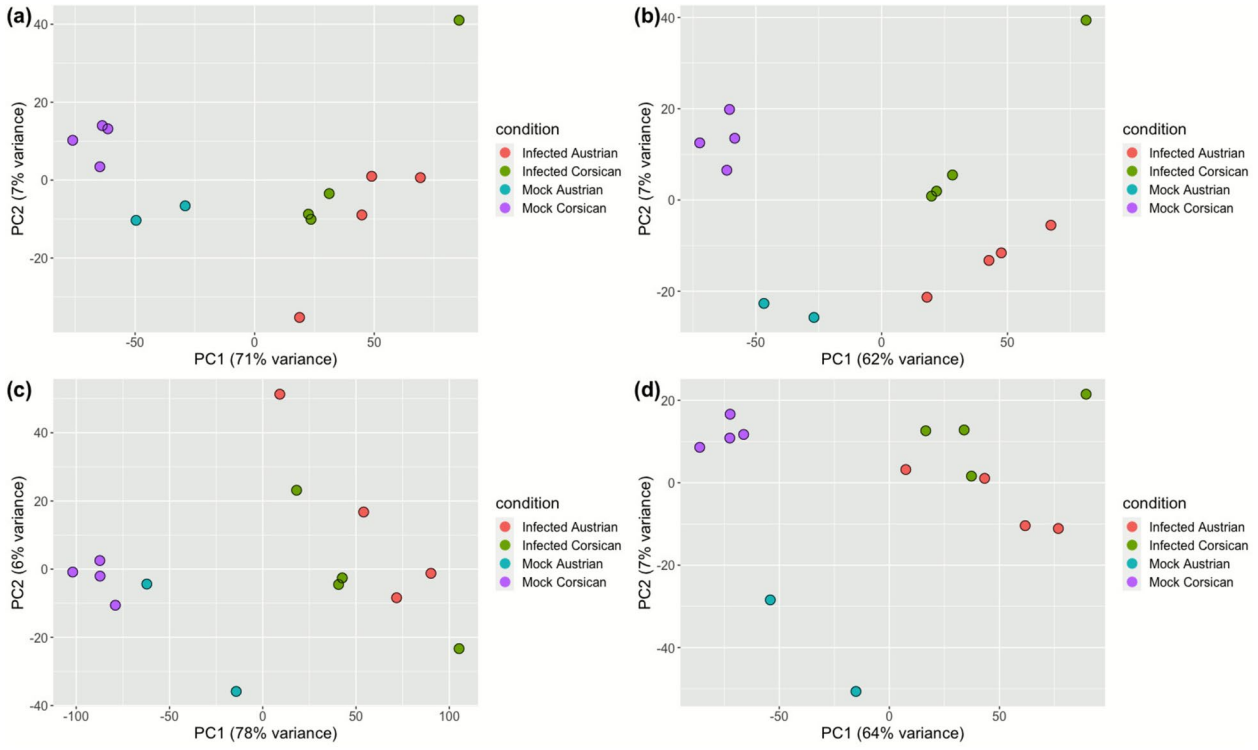

Fig. 2 Principal component analysis (PCA) plot of differentially expressed transcripts at 21 dpi (mRNA-seq). **a** BWA-MEM and (**b**) Salmon with *P. nigra* as reference transcriptome; **c** BWA-MEM and (**d**) Salmon with *P. sylvestris* as reference transcriptome. Note the high conformity within the four replicates (two for mock Austrian) and clear separation between mock and inoculated treatments at 21 dpi for both Austrian and Corsican saplings

Gene ontology (GO) enrichment analysis

The GO-enrichment analysis performed for the RELAXED gene set revealed terms significantly enriched (p-value < 0.05) for the three different gene ontologies explored: biological process (BP), molecular function (MF), and cellular component (CC) (Figure S4). For all categories and for both up- and down-regulated gene sets, there were fewer terms when the *P. sylvestris* transcriptome was used as reference instead of *P. nigra*. When using *P. nigra* as reference, many BP terms were enriched in the up-regulated gene set such as the chitin catabolic process, cell wall macromolecule catabolic process, and carbohydrate metabolic process. Interestingly, chitinase activity and chitin binding were the two most relevant MF here. In addition, defense response term was also enriched in this set, involving several related terms such as response to stress, to biotic stimulus, to oxidative stress, and to abscisic acid. Regulation of transcription was also enriched. For the down-regulated gene set, many terms related to cell wall architecture and organization were enriched, together with carbohydrate metabolic process, as well as some defense related terms such as response to biotic stimulus and oxidative stress. Nevertheless, when using *P. sylvestris* as reference, new terms emerged for the up-regulated gene set (i.e., response to auxin and desiccation, lipid metabolic process), although response to stress was also enriched. For the down-regulated gene set, again few terms appeared, most of them previously detected for *P. nigra*. Notably, a considerable proportion of differentially expressed genes remained without GO annotation.

Metabolic pathway analysis

The Kyoto Encyclopedia of Genes and Genomes (KEGG) pathway database was used as an alternative approach to categorize gene functions as it directly pinpoints specific and well-described biochemical pathways. On average, when the *P. nigra* sequences were used for the analysis, 17% of DEGs could be assigned to key enzymes involved in a total of 148 biological pathways, while 10% DEGs were assigned when *P. sylvestris* sequences were used (Table S3). DEGs were assigned to key enzymes of pathways involved in metabolism, genetic information processing, environmental information processing, cellular processes, and organismal systems; thus, constituting a pathway fingerprint (Table S4). In some cases, multiple genes were assigned to the same key enzymes, as expected due to genome complexity in conifers. Pathway fingerprints of both up- and down-regulated DEG sets were consistent and grouped together, irrespective of the reference transcriptome applied (Fig. 4a). At a more detailed level, provenances tended to group together but were more distinctly separated when the *P. nigra* reference was applied (Figure S5a). Finally, the alignment

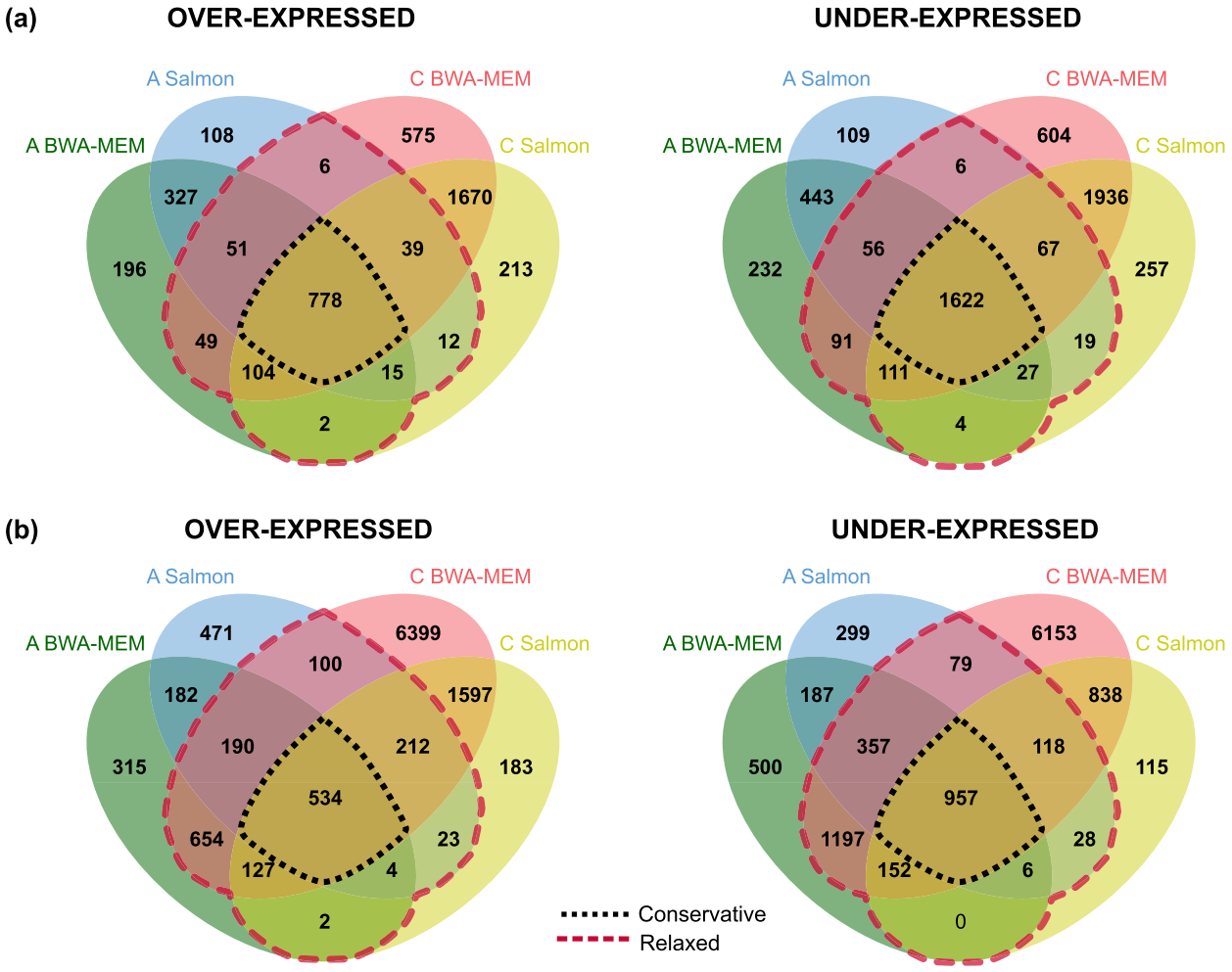

Fig. 3 Venn diagrams of up- and down-regulated transcripts in needles of *P. nigra* plants infected with *D. sapinea* compared to mock plants at 21 dpi. **a** DEGs for Austrian and Corsican samples detected both by BWA-MEM and Salmon when *P. nigra* was used as a reference transcriptome. **b** DEGs for Austrian and Corsican samples detected both by BWA-MEM and Salmon when *P. sylvestris* was used as a reference transcriptome. DEGs strictly shared between Austrian and Corsican samples for all alignment methods were considered CONSERVATIVE and are highlighted by a black dotted line. DEGs shared by at least a single alignment method by both provenances were considered RELAXED and are highlighted by a red dotted line. C and A abbreviations refer to Corsican and Austrian, respectively

method (BWA-MEM or Salmon) did not significantly change the pathway fingerprints. When RELAXED and CONSERVATIVE fingerprints were included, they integrated perfectly in the previously created hierarchy together with their relatives (Figure S5b). Moreover, they were generally comparable to the Austrian provenance, given that the Corsican provenance differed in certain specific pathways, as explained below.

When we focused on the RELAXED *P. nigra* alignment gene sets (Fig. 4b), the up-regulation found for most key enzymes and pathways involved in signal transduction and environmental adaptation such as plant-pathogen interaction, mitogen-activated protein kinase (MAPK) signalling and plant hormone signal transduction, all three crucial for the plant defense response (Table 1; Figure S6), is particularly notable. In addition, pathways such as protein processing, ribosome, pyruvate metabolism, glycerolipid metabolism and glycolysis/gluconeogenesis, clustered together again with most of their key up-regulated enzymes. On the contrary, down-regulated genes were mostly found in phenylpropanoid biosynthesis, the starting point for important plant secondary metabolite pathways such as flavonoids and stilbenes, which both follow similar trends. Likewise, key enzymes for amino sugar and nucleotide sugar metabolism, cutin, suberine and wax biosynthesis pathways, were mostly down-regulated. Finally, some systemic induced responses were provenance specific (Figure S7). Particularly, Corsican plants showed a clear up-regulation of some pathways (e.g., spliceosome and ribosome biogenesis) but an down-regulation of others (e.g., oxidative phosphorylation and phosphatidyl inositol).

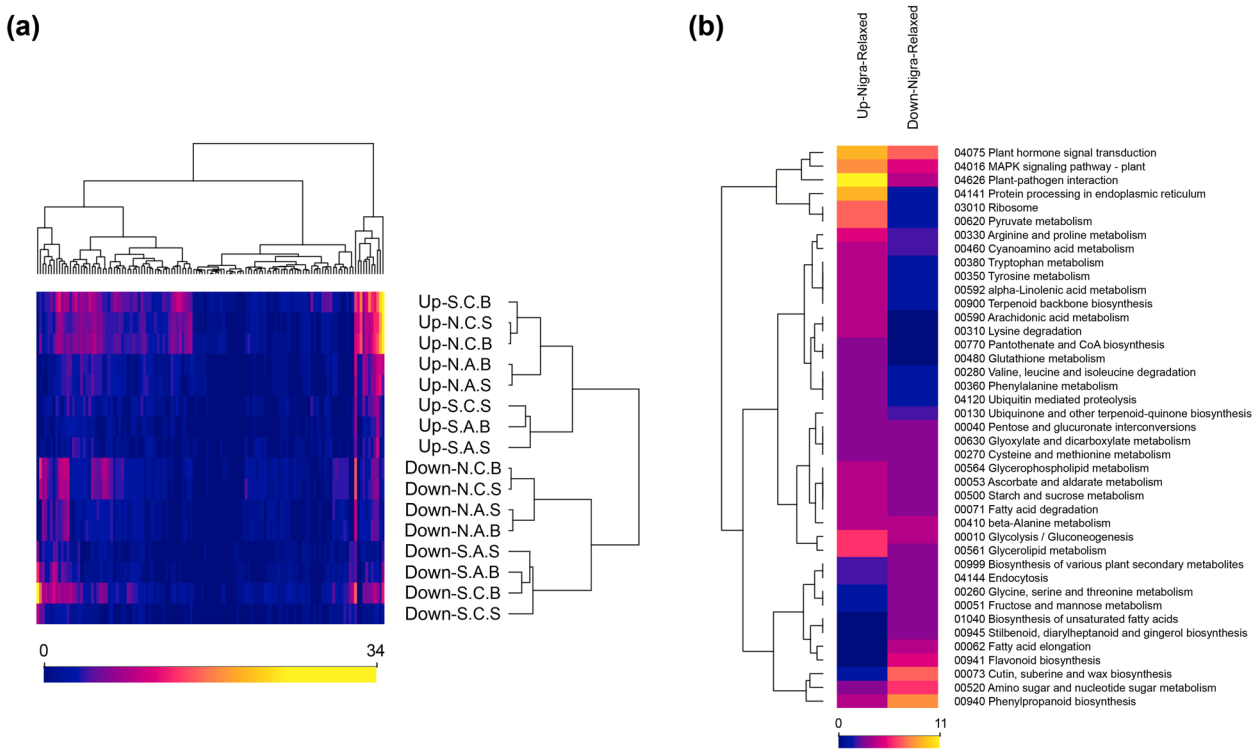

Fig. 4 Heat map for DEGs distribution among pathways (pathway fingerprint) showing the *P. nigra* induced defense response against *D. sapinea*. **a** The results revealed the similarity of all up- and down-regulated DEG fingerprints regardless of the reference transcriptome, provenance, and alignment method used. Pathways (columns) and DEG sets (rows) were sorted by clustering data by similarity using Euclidean distance as the distance metric. The number of enzymes represented within each pathway is shown using a color scale from blue (0) to yellow (34). Abbreviations are used to denote the different sets of DEGs obtained: "Up" and "Down" refer to the up- and down-regulated DEGs, followed by a letter referring to the reference transcriptome used (N: *P. nigra*; S: *P. sylvestris*), a second letter referring to the provenance (C: Corsican; A: Austrian), and a final letter referring to the alignment method used (B: BWA-MEM; S: Salmon). **b** Detailed view of the RELAXED gene set using the *P. nigra* transcriptome as reference. Underrepresented pathways (less than 3 differentially expressed key enzymes) were excluded to simplify the plot. Rows (pathways) were sorted by clustering using Euclidean distance as the distance metric. The number of enzymes represented within each pathway is shown using a color scale from blue (0) to yellow (11)

Changes in plant hormone and secondary metabolite concentrations

Plant hormones

Phytohormone concentrations were quantified in needles at 3, 8, and 21 dpi for both mock and inoculated plants. In the Austrian provenance inoculated plants, ABA, JA and SA contents were significantly increased at 21 dpi, while in Corsican provenance inoculated plants, a similar but smaller increase was observed for ABA and JA, but not for SA (Fig. 5). In addition, indole acetic acid (IAA) contents were significantly reduced at 8 and 21 dpi in the Corsican provenance (Table S5a). Regarding bioactive gibberellins (GAs), both GA_1 (13-hydroxylation pathway) and GA_4 (non-13-hydroxylation pathway) were detected, with GA_1 being the one with the higher concentration in the pine saplings. In the infected plants of Corsican provenance, GA_1 concentrations increased slightly at 21 dpi (Table S5a). In contrast, GA_4 levels were reduced in the infected plants across all time points, except at 21 dpi in the Austrian provenance, where GA_4 levels increased. In addition, some GA_1 intermediates and degradation products exhibited changes between mock and infected plants for both provenances (Table S5b). Finally, regarding cytokinins, the content of dihydrozeatin (DHZ) and trans-zeatin (tZ) decreased in Austrian and Corsican infected plants at 3 dpi. Nevertheless, there was a significant increase in the cytokinins from 21 dpi on in the Austrian inoculated plants (Table S5b).

Phenolic compounds and diterpenes

An untargeted LC–MS metabolomics analysis was performed in infected and mock needles. PCA of metabolic features showed a clear discrimination between Corsican and Austrian samples (Fig. 6a). Regarding the infection response, differences between infected and mock samples were evident at 21 dpi, suggesting that metabolic changes in response to infection started between 8 and 21 dpi. A hierarchical clustering additionally revealed three clear metabolic clusters (Fig. 6b). The first cluster included more than half of the metabolites and represented metabolites more abundant in Corsican samples. The second cluster included metabolites more abundant

Table 1 DEGs and pathways potentially involved in the induced defense response of *P. nigra* against *D. sapinea*. Here the log2FoldChange for RELAXED gene set, mapped by BWA-MEM using the *P. nigra* transcriptome as reference is presented

Pathway	KO Entry	Symbol	Name	DEG	log2FC (Austrian)	log2FC (Corsican)
A	K00864	glpK, GK	glycerol kinase [EC:2.7.1.30]	contig_16160	2.40	3.86
A	K04079	HSP90A, htpG	molecular chaperone HtpG	contig_1146	0.97	1.34
A	K05391	CNGC	cyclic nucleotide gated channel, plant	contig_14071	1.62	0.76
A	K12795	SUGT1, SGT1	suppressor of G2 allele of SKP1	contig_12852	-	0.57
A	K13412	CPK	calcium-dependent protein kinase [EC:2.7.11.1]	contig_15851	1.45	2.04
A	K13436	PTI1	pto-interacting protein 1 [EC:2.7.11.1]	contig_4613	1.44	1.25
A	K13448	CML	calcium-binding protein CML	contig_47666	3.53	3.56
				contig_37400	2.47	2.18
A	K18835	WRKY2	WRKY transcription factor 2	contig_8179	1.45	1.03
A	K13459	RPS2	disease resistance protein RPS2	contig_21507	-	−3.78
A	K15397	KCS	3-ketoacyl-CoA synthase [EC:2.3.1.199]	contig_62409	−1.84	−2.98
				contig_131560	−2.57	−4.50
				contig_55702	−2.78	−4.25
AB	K02183	CALM	calmodulin	contig_32952	1.59	1.29
				contig_31591	-	3.67
AB	K13420	FLS2	LRR receptor-like serine/threonine-protein kinase FLS2 [EC:2.7.11.1]	contig_39894	−3.14	−2.63
AB	K13447	RBOH	respiratory burst oxidase [EC:1.6.3.- 1.11.1.-]	contig_35666	−2.49	−1.87
ABC	K13449	PR1	pathogenesis-related protein 1	contig_19585	2.49	4.16
				contig_145314	2.46	4.27
ABC	K14512	MPK6	mitogen-activated protein kinase 6 [EC:2.7.11.24]	contig_14614	1.50	1.93
B	K00940	ndk, NME	nucleoside-diphosphate kinase [EC:2.7.4.6]	contig_37	1.27	0.71
B	K20547	CHIB	basic endochitinase B [EC:3.2.1.14]	contig_48603	2.69	4.96
				contig_26700	2.45	4.98
B	K17686	copA, ctpA, ATP7	P-type Cu + transporter [EC:7.2.2.8]	contig_36251	−3.14	−4.61
B	K20718	ER	LRR receptor-like serine/threonine-protein kinase ERECTA [EC:2.7.11.1]	contig_74606	−3.15	−2.14
BC	K13422	MYC2	transcription factor MYC2	contig_4910	1.44	1.76
BC	K14497	PP2C	protein phosphatase 2 C [EC:3.1.3.16]	contig_14511	2.30	1.51
BC	K14514	EIN3	ethylene-insensitive protein 3	contig_1279	0.83	0.74
BC	K14496	PYL	abscisic acid receptor PYR/PYL family	contig_65228	−1.30	−1.89
				contig_34927	−2.39	−2.99
C	K14488	SAUR	SAUR family protein	contig_38323	4.19	2.70
				contig_122884	3.62	3.17
				contig_583	−1.94	−1.73
				contig_149876	−4.27	−5.46
				contig_138431	−4.94	−4.06
				contig_35333	−1.70	−3.51
C	K13464	JAZ	jasmonate ZIM domain-containing protein	contig_14625	2.86	2.43
				contig_30296	2.11	2.86
				contig_78857	1.58	2.27
				contig_25662	1.15	0.96
C	K14493	GID1	gibberellin receptor GID1 [EC:3.-.-.-]	contig_10254	1.79	1.40
C	K14500	BSK	BR-signaling kinase [EC:2.7.11.1]	contig_124	1.22	1.27
C	K12126	PIF3	phytochrome-interacting factor 3	contig_428	−1.90	−1.20
C	K14484	IAA	auxin-responsive protein IAA	contig_66	−2.89	−2.99
				contig_22341	−1.61	−2.37
C	K14486	K14486, ARF	auxin response factor	contig_6742	−1.46	−0.91

Table 1 (continued)

Pathway	KO Entry	Symbol	Name	DEG	log2FC (Austrian)	log2FC (Corsican)
C	K14489	AHK2_3_4	arabidopsis histidine kinase 2/3/4 (cytokinin receptor) [EC:2.7.13.3]	contig_1115	−1.75	−1.59
C	K14490	AHP	histidine-containing phosphotransfer peotein	contig_76203	−3.66	−4.09
D	K00430	E1.11.1.7	peroxidase [EC:1.11.1.7]	contig_15839	3.65	3.86
				contig_95	3.04	4.07
				contig_8081	2.61	2.12
				contig_114322	−1.94	−2.79
				contig_132621	−3.68	−2.97
				contig_39622	−4.15	−3.77
				contig_77181	−4.27	−5.78
				contig_131928	−5.66	−8.87
				contig_132175	−5.99	−4.88
				contig_131438	−8.76	−5.20
				contig_15496	-	−3.27
D	K10775	PAL	phenylalanine ammonia-lyase [EC:4.3.1.24]	contig_52979	2.49	3.51
				contig_5606	−3.76	−4.38
D	K18368	CSE	caffeoylshikimate esterase [EC:3.1.1.-]	contig_25864	1.67	3.11
D	K22395	K22395	cinnamyl-alcohol dehydrogenase [EC:1.1.1.195]	contig_49986	3.14	3.99
D	K01904	4CL	4-coumarate–CoA ligase [EC:6.2.1.12]	contig_37952	−2.11	−1.72
D	K09753	CCR	cinnamoyl-CoA reductase [EC:1.2.1.44]	contig_131640	−4.24	−4.20
				contig_132656	−3.08	−3.17
D	K13066	COMT	caffeic acid 3-O-methyltransferase/ acetylserotonin O-methyltransferase [EC:2.1.1.68 2.1.1.4]	contig_128943	−2.36	−3.45
DE	K00487	CYP73A	trans-cinnamate 4-monooxygenase [EC:1.14.14.91]	contig_9871	−1.79	−1.99
DE	K00588	E2.1.1.104	caffeoyl-CoA O-methyltransferase [EC:2.1.1.104]	contig_10359	−1.11	−1.13
DE	K13065	E2.3.1.133, HCT	shikimate O-hydroxycinnamoyltransferase [EC:2.3.1.133]	contig_48805	−4.90	−4.40
E	K05277	ANS	anthocyanidin synthase [EC:1.14.20.4]	contig_34335	−3.54	−3.94
E	K08695	ANR	anthocyanidin reductase [EC:1.3.1.77]	contig_10613	−1.88	−2.12

A Plant-pathogen interaction, *B* MAPK signaling pathway—plant, *C* Plant hormone signal transduction, *D* Phenylpropanoid biosynthesis, *E* Flavonoid biosynthesis

in Austrian samples, and the third cluster included metabolites induced upon infection in both provenances.

After filtering from a possible 899 features, 77 metabolites were retained for further consideration (Table S6; Fig. 6c). The metabolic clustering of these 77 metabolites, shown in Fig. 6c, is similar to the one based on the raw data (Fig. 6b). The identified metabolites fell into the main classes of phenylpropanoids previously identified in conifers (reviewed by [65]), namely flavonoids, hydroxybenzoic and hydroxycinnamic acids, proanthocyanidins, lignans, and stilbenes. Corsican samples were richer in flavonoids and glycosylated hydroxycinnamic acids, whereas Austrian samples contained higher levels of proanthocyanidins and lignans. In our untargeted LC–MS analysis, diterpene resin acids were also identified, with higher accumulation in Corsican samples.

Among the 25 metabolites with increased accumulation upon infection by *D. sapinea*, the most represented families were flavonoids (16 metabolites) and hydroxycinnamic acids (5 metabolites). Both aglycons and conjugated forms (glycosylation and coumaroyl glycosylation) were identified.

Volatile organic compounds (VOCs)

A total of 43 VOCs were identified in *P. nigra* needles: 6 fatty acid-derived VOCs, 21 monoterpenoids, and 16 sesquiterpenoids (Table S7). A PCA analysis revealed that the distribution of VOCs differed between provenances (Figure S8a). In contrast to the phenolic distribution, infection did not significantly change the terpenoid content (Figure S8a). Nevertheless, a hierarchical cluster analysis (Figure S8b) showed that Corsican samples contained higher levels of monoterpenoids and a group of

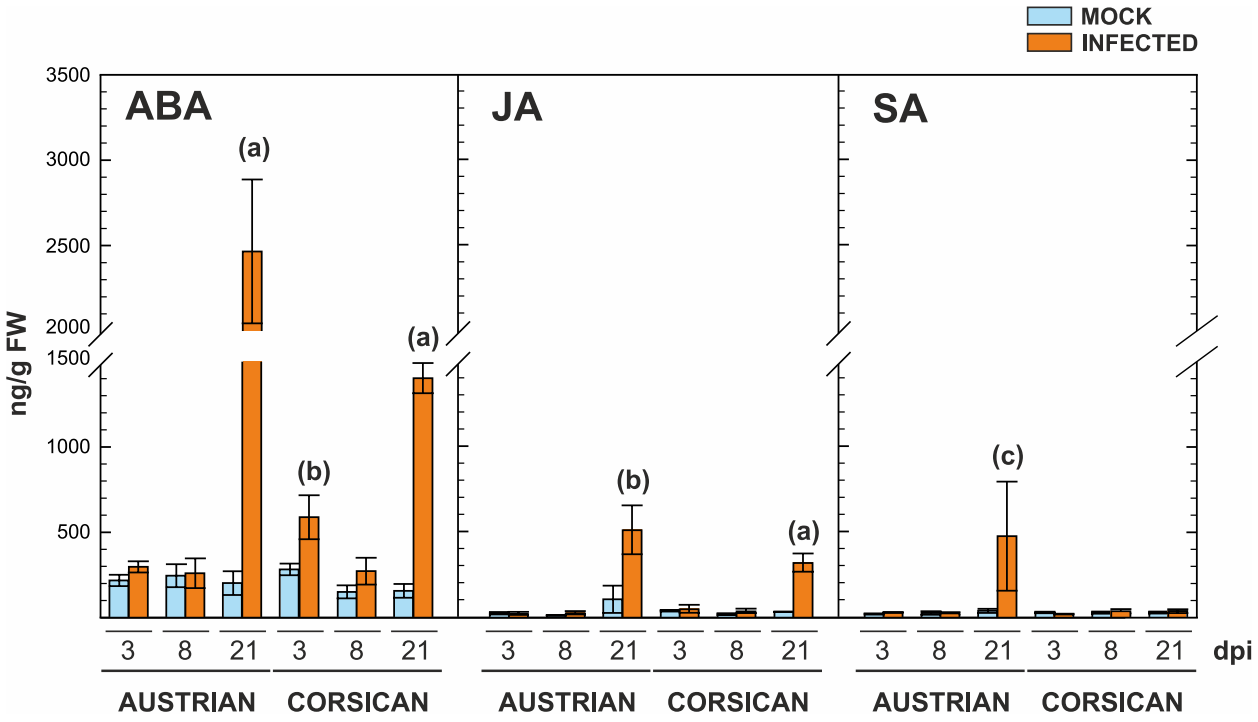

Fig. 5 Abscisic acid (ABA), jasmonic acid (JA), and salicylic acid (SA) hormone concentrations in needles of infected and mock plants of Austrian and Corsican *P. nigra* provenances at 3, 8, and 21 dpi. Data are presented as mean ± standard error (SE), $N = 4$. Significantly different values are indicated with letters [($p < 0.001$ (a); $p < 0.005$ (b); $p < 0.01$ (c)]

sesquiterpernoids (alpha- and beta-selinene, alpha- and tau-cadinol, beta-elemene, and alpha and beta-caryophyllene). The remaining VOCs (fatty acid-derived and a second group of sesquiterpenoids: alpha-and gamma-muurolene, gamma-cadinene, alpha-amorphene, alpha and beta-copaene, germacrene and cubebene) showed higher variation among individual plants than between groups.

Discussion

Much remains unknown about the defense mechanisms of conifers against pathogens compared to model species (e.g., *Arabidopsis thaliana* (L.), Heynh) and crop plants (e.g. *Zea mays* L.). Although previous studies have investigated the response of *P. nigra* and other pine species to *D. sapinea* [29, 44, 46, 62], this study presents a novel investigation of the molecular responses of two—Austrian and Corsican—*P. nigra* provenances by combining transcriptomics and metabolomics. Doing so builds on the previous success of this approach in revealing host plant molecular defense mechanisms against pathogens [9, 46, 56, 57, 66]. Wound inoculation of *P. nigra* plants with *D. sapinea* during shoot elongation was effective in all inoculated plants at the end of the experiment, as confirmed both phenotypically and by the RT-qPCR general host response. The latter was monitored using 21 *P. nigra* defense-related candidate genes that showed the greatest induced expression at 21 dpi, making this time point the most interesting to explore further by sequencing; a time point previously unexplored by recent studies on this pathosystem [44, 52]. The adaptation and redesign of primers for both housekeeping genes and candidate genes from other closely related species facing the same pathogen [62] or other distant conifer pathosystems [57] was relatively simple and effective due to the availability of the *P. nigra* transcriptome [63]. RT-qPCR is shown here to be a very useful tool for investigating multiple time points in this pathosystem in a cost-effective and rapid manner prior to RNA-seq and may also be useful in other conifer pathosystems where only limited genomic information is available.

Utility and limitations of the *P. nigra* transcriptome

The *P. nigra* transcriptome was useful for primer adaptation and gene expression analyses of specific genes along the process. However, a rather low proportion of mapped reads in this study indicated a limitation of its use in RNA-seq experiments. At the start of this study there were no closely related reference genomes available, and the transcriptomic references used (*P. nigra* and *P. sylvestris*) are incomplete as they represent a subset of expressed genes. The higher mapping rate of reads achieved for *P. sylvestris* (85%) than for *P. nigra* (53%) could be explained by differences in the experimental tissue type and life stage used to generate the transcriptomes (see Introduction [56]). This highlights the need

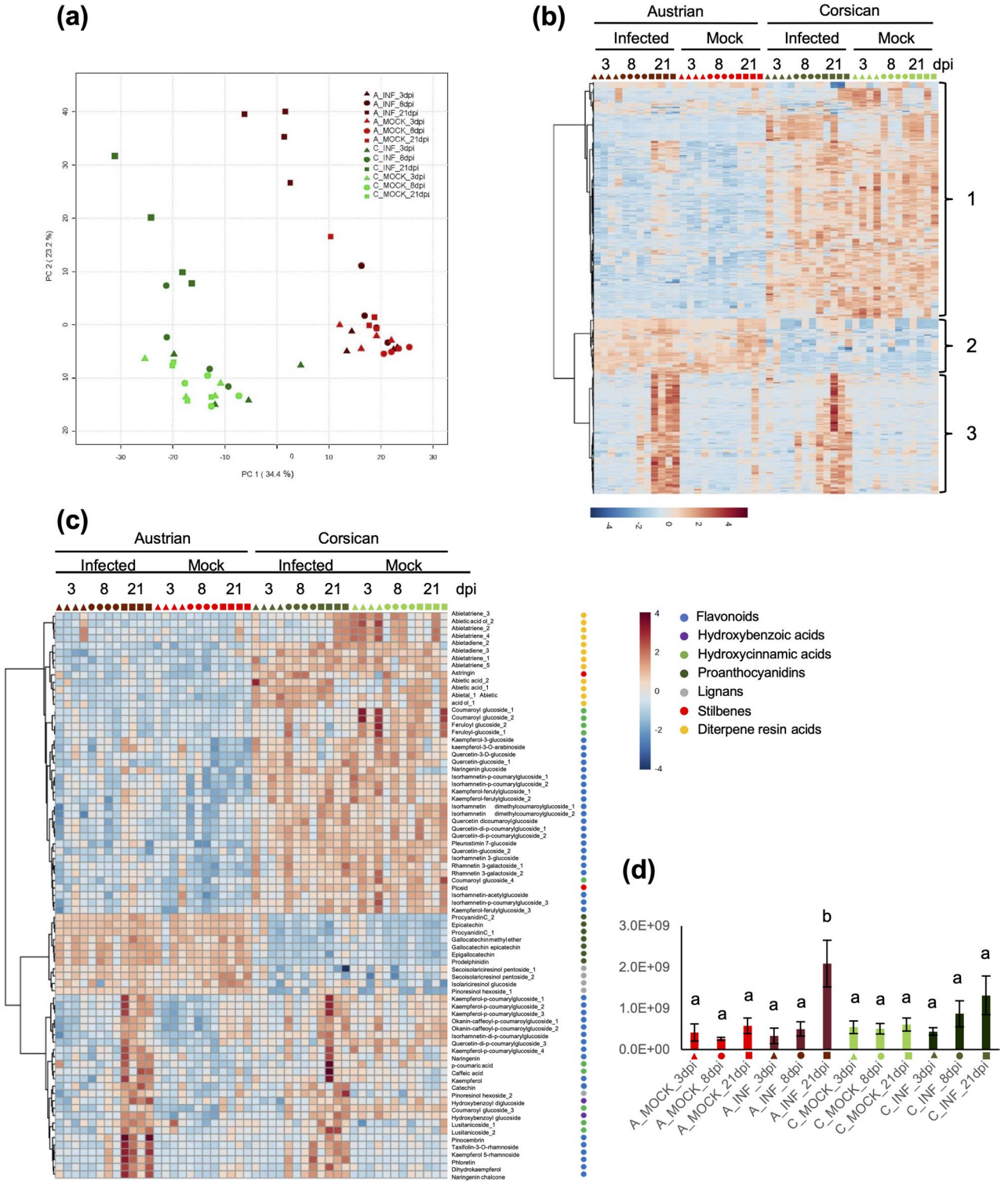

Fig. 6 Phenolic compounds identified in *P. nigra* needles upon infection by *D. sapinea*. **A** Principal component analysis (PCA) of the 889 metabolic features identified in the LC–MS untargeted analysis. Green is used for Corsican samples and pink for Austrian samples. **B** Hierarchical cluster analysis of the 889 metabolic features identified in the LC–MS untargeted analysis. Colors in the heat map represent the Z-fold. **C** Hierarchical cluster analysis of the 77 metabolites identified after manual curation. Colors in the heat map represent the Z-fold. **D** Sum of areas (TIC, total ion current) of cluster 3 metabolites in mock and inoculated samples at the different time points (3,8, 21 dpi). Letters indicate significant differences after ANOVA and post-hoc Tukey test ($p < 0.01$)

for complete well-annotated conifer genomes, particularly for *P. nigra*. The choice of alignment method also influenced mapping efficiency. While BWA-MEM and Salmon are both appropriate aligners for the very short read lengths used in RNA-seq gene expression profiling [67], such as in our study, BWA-MEM clearly yielded more mapped reads than Salmon. As these mapping tools use different approaches, their total mapping percentages are not directly comparable. The differences in the method performance align with previous studies on transcript abundance estimation [68]. However, determining the optimal approach remains challenging, as real-life cases might greatly vary and differ substantially from simulated data.

Notably, RNA sequencing detected *D. sapinea* sequences even in mock plants, supporting previous findings that this pathogen can be widespread in asymptomatic trees (e.g. [69]). Despite this unexpected detection, our data interpretation remained unchanged, as systemic induced responses took effectively place evidenced phenotypically and molecularly by elevated JA levels, subsequent marked differential expression, and pronounced metabolomic shifts (all discussed below). These findings raise important ecological questions about the latent infection dynamics of *D. sapinea* and the environmental conditions that may trigger its pathogenicity.

RNA-seq findings and differential gene expression

RNA-seq revealed a large number of DEGs between mock and inoculated trees at 21 dpi. Regardless of the reference transcriptome (*P. nigra*, *P. sylvestris*) and the alignment method applied (BWA-MEM, Salmon), similar transcriptional patterns were found for both Austrian and Corsican provenances, with a large proportion of shared transcripts and a slight trend towards down-regulation. The greater distance between the Austrian mock samples when *P. sylvestris* was used as the reference could be due to specific genes that are not easily detected against the cross-species reference, but which were better captured against the *P. nigra* reference. The availability of only two Austrian mock samples could cause type I errors in DEG identification. However, the expression changes detected by RNA-seq were validated for almost all the transcripts using RT-qPCR without the need for further DEGs validation. A large set of genes shared by at least one alignment method across both provenances represented the general response of *P. nigra* to *D. sapinea* inoculation. Obtaining gene ontologies (GO) and KEGG pathways (KO) through the annotation step were crucial for performing enrichment analyses on the DEGs, but despite using multiple databases for annotation, a significant proportion of genes remained unannotated. Unfortunately, this problem is not easily solved as experimental studies on conifers are still limited and annotations are generally obtained from model organisms such as *Arabidopsis*, which are not closely related to conifers. This has a significant impact on the results and affects all studies on conifers (e.g. [70].

Using the *P. nigra* transcriptome as a reference, an overall analysis of GO enrichment terms for the RELAXED gene set revealed numerous differentially regulated genes related to plant defense responses to biotic stimuli and subsequent oxidative stress (Figure S4). Moreover, the enriched terms found in the up-regulated gene set show that the defense response enhances the chitin catabolism and chitinase activity. Chitin is a well-known target of plant defense ammunition to combat fungal diseases, as it is the key component of fungal cell walls [44, 46]. In addition, the response to abscisic acid—also enriched here—highlights the essential role of this phytohormone in the defense response (discussed further below). Primary metabolism, including carbohydrate metabolic processes, also appears to be crucial here, as it appears to be enriched in the up and down-regulated gene sets. In addition, the down-regulated gene set was enriched for many GO terms related to cell wall architecture and organization, together with some plant secondary metabolisms, including lignin catabolism and flavonoid biosynthesis processes, making plant secondary metabolites fit for the defense needs. Alternatively, when the *P. sylvestris* transcriptome was used as a reference, fewer terms were enriched, possibly because species-specific genes were missed, and only more general processes were detected.

The KO analysis, although limited here due to the low number of annotated genes compared to conifers with a complete reference genome available [57], allowed for the identification of the most important conserved key genes and pathways potentially involved in the plant defense response of *P. nigra* against *D. sapinea*. Hierarchical clustering of pathway fingerprints clearly showed that RELAXED gene sets retained the most conserved genes from the current transcriptomes for both up- and down-regulated DEGs. The increased divergence observed between provenances when using the *P. nigra* reference (compared to *P. sylvestris*) is likely due to the higher resolution and specificity of the *P. nigra* transcriptome, which captures more provenance-specific variation. In contrast, the *P. sylvestris* reference primarily reflects conserved sequences at lower resolution. This was expected as the *P. nigra* reference is not a single sample reference transcriptome, but rather a transcriptomic resource comprised of six geographically distinct samples from five different subspecies [63]. Despite the significantly reduced alignment rate when using *P. nigra* as a reference compared to *P. sylvestris*, the pathway fingerprints derived from the DEGs were equivalent and the most important genes were retained for appropriate in-depth downstream pathway analysis. This result led us to further focus on

the pathway fingerprint derived from the *P. nigra* reference transcriptome (Fig. 4). The analysis indicated that the major response genes and pathways may be shared between the provenances and that there are some provenance-specific pathways that are differentially expressed (Figure S7). These findings confirm our hypothesis that *D. sapinea* stem inoculation of two-year seedlings triggers systemic induced reactions in the terminal shoot needles, encompassing both shared and provenance-specific reactions.

Key defense-related pathways and secondary metabolite shifts

Overall, a large number of up-regulated genes (coding for key enzymes) were found in pathways involved in signaling and environmental adaptation, including plant-pathogen interaction, MAPK signaling and plant hormone signaling (Table 1, Table S4, Figure S6). These interconnected pathways (with shared key genes) are critical for the plant defense response, as they are involved in pathogen recognition and the activation of other pathways that adapt plant metabolism and physiology to the challenge [44]. The major signaling hormones boosted and involved in this process were ABA and JA, as previously described in a closely related pathosystem [37, 45]. ABA is strongly associated with drought stress signaling, but it appears that infection with *D. sapinea* results in a similar host response, as suggested also by previous studies [46], anticipating the final stage of this disease of a dry, necrotic shoot/stem. Interestingly, SA is also relevant here, but its importance may vary in different provenances, such as between Austrian and Corsican. Differentially regulated genes from the plant-pathogen interaction pathway were involved in both interlinked immune systems: pattern-triggered immunity (PTI) and effector-triggered immunity (ETI) (Figure S6a). The expression of two pathogenesis-related protein 1 (PR1) genes, contig_19585 and contig_145314, increased as a result of gene expression promoted by these pathways. These defense proteins are known to be induced in response to various pathogens, to mount an efficient immune response against pathogen attack [44, 71], and to act as markers for salicylic acid-mediated disease resistance [72] among other functions. Additionally, within the MAPK signaling pathway, mitogen-activated protein kinase 6 (MPK6), represented by contig_14614, plays a crucial role in plant disease resistance and is involved in multiple signaling pathways [73, 74]. Research has shown that there is a complex interaction between the MAPK cascade and hormone signaling pathways in plant defense [75], with MPK6 amplifying defense signals and regulating downstream defense-related genes, including those involved in JA biosynthesis [76] (Figure S6bc). The elevated JA levels activate the transcription factor MYC2, represented by contig_4910, which facilitates defense responses by regulating the expression of various genes [77, 78], including basic endochitinases B (contig_26700 and contig_48603). Well known defense proteins that offer effective defense against chitin-containing fungal pathogens [79–81]. These findings provide further evidence of the conservation of pathways and genes in conifers, as demonstrated by the consistent patterns observed in selected genes for RT-qPCR across equivalent [62] and different conifer-fungal pathosystems [57].

As a master regulator of JA-responsive genes, MYC2 plays a pivotal role in JA signaling, further amplifying its impact on orchestrating plant defense responses, particularly those involving the biosynthesis of plant secondary metabolites (Figure S6d-f). The phenylpropanoid biosynthetic pathway, responsible for the production of important plant secondary metabolites such as flavonoids, stilbenes, tannins, coumarins, lignans, and others, showed mostly down-regulated genes (Table 1, Fig. 6). Genes involved in lignin biosynthesis were mostly down-regulated, apart from a cinnamyl-alcohol dehydrogenase (contig_49986) and a caffeoylshikimate esterase (contig_25864). In addition, down-regulation of 8 out of 11 peroxidases may have reduce lignin formation [82]. Consequently, a decreased flux to the lignin pathway could explain the observed accumulation of hydroxycinnamic acids following the infection by *D. sapinea*. However, experimental evidence confirming this reduced flux in lignin formation will be essential to validate the hypothesis. In addition, the flavonoid biosynthetic pathway also showed down-regulation of the anthocyanidin synthase (contig_34335) and the anthocyanidin reductase (contig_10613), which may hinder the biosynthesis of anthocyanidins and related products such as anthocyanins and tannins. These data agree with the observation that flavonoids, upstream from anthocyanidins, also accumulate upon infection. As a result, the metabolic profiles of the inoculated plants shifted towards the accumulation of hydroxycinnamic acids (p-coumaric and caffeic acid) and flavonoids (kaempferol, naringenin, pinocembrin, phloretin, naringenin chalcone, dihydrokaempferol and catechin), as previously described by [48]. Notably, the absence of stilbene accumulation in response to infection is striking, despite this response being well-described in the literature for this pathosystem [49] and others [83]. Finally, inoculation had no significant effect on terpenoid content in the needles of any of the provenances studied (Figure S8a), contrary to what was observed on the phloem [49, 52]. Nevertheless, similar to the phenolic profiles, constitutive differences between the provenances were observed, which is consistent with known oil composition across different subspecies of *P. nigra*, including terpenoids [84, 85].

By integrating transcriptomic and metabolomic analyses, our findings align with our hypothesis that systemic induced responses in needles include significant changes in stress-related phytohormone profiles that trigger plant defense signaling pathways, and subsequent differential gene expression that coincides with significant changes in defense proteins and phenolic compounds. The correlogram confirmed the strong correlations discussed above between hormones, key DEGs from signal transduction and environmental adaptation pathways, as well as DEGs from plant secondary metabolite biosynthetic pathways and induced secondary metabolites (Figure S6g).

Ultimately, we have identified key genes and metabolic pathways involved in the induced defense response—an insight that will be critical for genetic studies linking resistance or susceptibility to *D. sapinea* with specific genetic variants.

Future research perspectives

This study advances significantly the integration of gene expression, metabolomics, and hormonal analyses. However, several aspects warrant further research. (a) Transcriptomic analyses highlight the need for a robust genomic reference for expression studies. Expanding current transcriptomic references or developing a complete reference genome with appropriate annotation would improve the accuracy of similar studies. An additional avenue worth exploring is the evaluation of the recently published *P. tabuliformis* genome [86] for its applicability to *P. nigr*a and other pine species. (b) Molecular characterization of the DEGs involved in the induced defense response, combined with analysis of sequence variation (e.g., SNPs) across *P. nigra* subspecies and provenances, is crucial for identifying molecular markers linked to resistant genotypes (either constitutive or SIR), in genome-wide association studies (GWAS) for breeding purposes. To streamline such efforts, standardized protocols for mass screening of *P. nigra* resistance to *D. sapinea* under controlled conditions are needed, along with studies on constitutive and inducible defense differences at the RNA and metabolomic levels. (c) The isolation and sequencing of *D. sapinea* strains with varying levels of virulence [87] will support the selection of the appropriate virulent inoculum for resistance screening across *P. nigra* provenances. This approach would facilitate the identification of the most resistant genotypes for breeding programs. (d) Advancing our understanding of the molecular mechanisms underlying the endophytic behavior of *D. sapinea,* including its tissue-specific localization and its spread within the host and the environmental triggers that shift it from a latent to a pathogenic phase. Abiotic stressors such as drought [2, 27, 43], hail [88] or changes in soil nitrogen concentration [25, 89] can weaken host resistance, thereby facilitating infection either by *D. sapinea* or by co-occurring pathogens [53].

Conclusions

This study provides novel insights into the defense mechanisms of *P. nigra* against the pathogen *D. sapinea*. By combining transcriptomics and metabolomics, the study identified key molecular responses in two *P. nigra* provenances (Austrian and Corsican) during *D. sapinea* infection. The findings highlight the effectiveness of RT-qPCR for monitoring gene expression and suggest its usefulness in other conifer pathosystems with limited genomic information. However, the study also revealed limitations in the current *P. nigra* transcriptome reference and the need for a complete reference genome for this forest tree species. RNA-seq analysis effectively detected differential gene expression between mock and infected trees at 21 dpi, most of them shared by both Austrian and Corsican plants. Pathway analysis identified conserved key genes and pathways related to plant defense response, including plant-pathogen interaction, MAPK and plant hormone signaling (PR1, MPK6, MYC2, endochitinases among others). Hormones such as JA and ABA were found to play important roles in the defense response, and genes involved in the PTI and ETI pathways were up-regulated. Moreover, the study observed changes in secondary metabolite biosynthesis, including the accumulation of specific flavonoids and hydroxycinnamic acids in response to infection. However, stilbenes and VOCs were not induced upon inoculation, despite their documented role in other pathosystems. This systemic induced defense response and its nature agree with our initial hypotheses. Overall, this study enhances our understanding of the defense molecular mechanisms employed by *P. nigra* against *D. sapinea* and provides valuable insights for future research in this and other conifer pathosystems. Further exploration of the different subspecies and provenances with varying constitutive and induced defense responses against *D. sapinea* will be helpful to fully understand the dynamics of this pathogen.

Experimental procedures

Plant material and study design

Potted two-year-old black pine (*Pinus nigra*) saplings (180 plants) from two different open-pollinated provenances—Austria (*P. nigra* subsp. *nigra*, seed stand: Hernstein 7(5.1/sm), coordinates: 47.90N, 16.14E,) and Corsica (*P. nigra* subsp. *laricio*, seed stand: PLO902, seeds provided from Vilmorin (www.vilmorin-tree-seeds.com), coordinates: south-west France, artificial stands, privacy policy)—grown under identical conditions, were purchased from the commercial forest nursery (LIECO GmbG & Co KG) and repotted into 1L pots in the forest

garden of the Austrian Research Centre for Forests (BFW, coordinates: 48.17N, 16.30E,), in Vienna, Austria. The entire experiment took place at this location. The terminal shoots of all saplings were measured to enable the selection of 48 individuals with similar shoot length from both provenances (159 ± 15 mm Austrian, 149 ± 18 mm Corsican) and thereby ensure biological uniformity. Prior to the treatments, these were further randomly divided into two groups of 24 saplings for mock and inoculation, respectively.

Diplodia sapinea cultivation, preparation of the inoculum

The *D. sapinea* strain used for inoculation was isolated from symptomatic, current-year shoots of *D. sapinea*-infected black pine trees in Austria (Austrian *D. sapinea* strain EGY V/2 (2018)). Needles were removed from the shoots, and sterilized in 96% EtOH (1 min), 4% NaOCl (3 min), and finally in 96% EtOH (30 s). Afterwards, 5 mm long pieces were cut out under sterile conditions and placed on Bavendamm medium (10 g agar–agar, 2.4 g malt extract, 2.4 g tannic acid per 500 ml water, adjusted to a pH above 8.6 before autoclaving to ensure solidification of the medium), which is fairly selective for *D. sapinea*. Petri dishes were kept at room temperature and monitored regularly during the following days for the development of *D. sapinea*. If greyish mycelium resembling *D. sapinea* appeared, pieces of mycelium were transferred to fresh Bavendamm medium plates. To stimulate development of fruiting bodies, autoclaved black pine needles were placed on the medium surface and after one week of growth the petri dishes were then exposed to near UV light (350–400 nm). Once fruiting bodies appeared, cultures could be identified as *D. sapinea* according to culture morphology as well as morphology of fruiting bodies and conidia. Morphological identification was further confirmed by molecular identification using PCR (Figure S9). DNA was extracted from fungus cultures by adding 50 mg mycelium to a ZR BashingBead Lysis Tube (2.0 mm) filled with 750 µl BashingBead Buffer (Zymo Research, Irvine, CA, USA) followed by homogenization on a MagNA Lyser instrument (Roche, Rotkreuz, Switzerland) at 7000 rpm for 90 s and DNA isolation with the Quick-DNA Plant/Seed Miniprep Kit (Zymo Research). PCR for *D. sapinea* and *D. scrobiculata* was done using species-specific PCR assays [32]. PCR reactions were conducted in 50 µl volumes including 0.2 mM of each dNTP, 1 × Buffer B2, 2.5 mM $MgCl_2$, 1.25 units HOT FIREPol DNA Polymerase (Solis BioDyne, Tartu, Estonia), 300 nM of each primer and 20 ng DNA template. The PCR temperature profile was conducted as described [32], except for the elongation of the initial denaturation step to 12 min at 95 °C, to activate the hot-start polymerase. PCR products were visualized using D1000 ScreenTapes on a 4200 TapeStation system (Agilent, Santa Clara, CA, USA).

Infection protocol

Inoculation treatment via inoculation under the bark flap was carried out during the period of shoot elongation and needle unfolding, a prerequisite for successful symptom development. The treatment involved inserting an agar cube (≈ 4 × 4 mm) into a bark flap cut with a scalpel on the current year's terminal shoot approximately 1 cm from the shoot base. The flap was then closed again and wrapped with parafilm to prevent desiccation. In pathogen-inoculated plants, the agar cube contained mycelium of *D. sapinea*, while agar cubes without *D. sapinea* were used for the mock controls. For the duration of the experiment—May to September 2020—the plants of both provenances were regularly watered and kept in random order in two foil greenhouses, one containing the mock plants, and the other one contained *D. sapinea* inoculated plants. After 21 days post-inoculation (dpi), all saplings inoculated with *D. sapinea*, from both Austrian and Corsican provenances, exhibited clear symptoms of infection. This included curling of the shoot tips, an early stage preceding the development of the characteristic "shepherd's crook" shape when the shoot ultimately dies. In contrast, mock plants showed no symptoms throughout the entire infection experiment (Figure S10) nor after 21 dpi.

Sampling

Plant material—all needles from the current-year terminal shoot—was always collected in the morning and stored in RNase-free tubes. The distance of sampled needle tissue from the inoculation site ranged from 1 cm at the base of the terminal shoot to 15 cm for at the top. Samples were collected at 3, 8, and 21 dpi for all sample groups (mock Austrian, infected Austrian, mock Corsican, infected Corsican) with a total of 4 biological replicates sampled per treatment. Samples were immediately frozen in liquid nitrogen and stored at −80 °C until further analysis. Downstream molecular analysis (described below) for all samples consisted of RT-qPCR, identification and quantification of plant hormones, phenolic compounds, diterpenes and VOCs. The RNA-seq was analyzed for the 21-dpi instant only.

RNA extraction

Twenty frozen pine needles were added to a ZR BashingBead Lysis Tube (2.0 mm) (Zymo Research) supplemented with 800 µl Lysis Solution and 8 µl 2-Mercaptoethanol (Sigma-Aldrich, St. Louis, MO, USA) and homogenized on a MagNA Lyser instrument (Roche) at 7000 rpm for 30 s. RNA extraction was conducted according to Protocol B of the Spectrum Plant Total

RNA Kit (Sigma-Aldrich) including a DNase digestion step with the On-Column DNase I Digest Set (Sigma-Aldrich). RNA concentrations were measured on the DS-11 FX + spectrophotometer (DeNovix, Wilmington, DE, USA). RNA integrity numbers (RIN) were assessed on a 4200 TapeStation system with the RNA ScreenTape assay (Agilent).

RT-qPCR

Twenty-one *P. nigra* orthologs were selected for RT-qPCR analysis: 18 *P. sylvestris* genes which were up-regulated when infected by *D. sapinea* [62], and 3 *P. abies* genes which were up-regulated when infected by *Chrysomyxa rhododendri* [6, 57]. *Blastn*, *megablast* and *tblastx* [90] with default setup on *Geneious Prime 2021.1.1* software https://www.geneious.com) were used to find ortholog transcripts from the *P. nigra* reference transcriptome [63]. Primers from *P. sylvestris* [62] and *P. abies* [57] were then used for amplification when possible, applying slight modifications when necessary. The same approach was used for the primer design of 4 candidate reference genes (RGs): α-Tubulin [62], ACT, ATUB and UBI [57].

The following defined parameter values were applied for new primer design: Length of primers = 18–22 bp, T_m = 50–65°C, CG content = 40–60%, no hairpin, and self and pair dimer or T_m below primer T_m. The final set of primers was tested by using the "Extract PCR Product" function in *Geneious Prime* to confirm the reference specificity [63] and formation of a unique virtual product of the expected size. Primer sequences and PCR reaction efficiencies are listed in Table S8.

For RT-qPCR, 1 µg total RNA were used for reverse transcription (RT) with the SuperScript III First-Strand Synthesis SuperMix (Invitrogen, Carlsbad, CA, USA) and oligo (dT) primers according to the manufacturer's protocol. No RT controls (without RT enzyme) were included to monitor for contaminant DNA. RT-qPCR reactions were adjusted to a total volume of 20 µl including 1 × HOT FIREPol EvaGreen qPCR Mix Plus (ROX) (Solis BioDyne, Tartu, Estonia), 200 nM of each primer and 25 ng cDNA. Samples were analyzed in duplicates on a qTOWER^3 G real-time PCR cycler (Analytik Jena, Jena, Germany) with the following temperature conditions: 95 °C for 12 min, 40 cycles of 95 °C for 15 s and 60 °C for 1 min, followed by a melting curve analysis step (60 °C – 95 °C). The expression stabilities of the four candidate reference genes (RGs), namely α-Tubulin, ACT, ATUB and UBI, were evaluated using the RefFinder tool on a subset of the samples [91]. Actin and ATUB were identified as the two most stably expressed genes and selected for normalization. Target Cq-values were corrected for the PCR reaction efficiencies and normalized to the geometric mean of both RGs. Fold changes were calculated with the comparative $2^{-\Delta\Delta CT}$ method [92]. Statistical analyses (two-tailed unpaired t-test with Welch's correction) were performed with GraphPad Prism 8.4.3 software (GraphPad Software, San Diego, CA, USA). A p-value of < 0.05 was considered significant.

Library preparation, pooling, and sequencing

Twenty-one dpi samples stored at −80 °C were processed at Lexogen GmbH (Vienna, Austria). Concentration of the samples was analyzed by UV–Vis spectrophotometry (Nanodrop 2000c; Thermo Fisher Scientific, Waltham, MA, USA), and RNA integrity was assessed using Fragment Analyzer (Agilent). Libraries for sample subset were prepared manually according to the user guide (015UG009V0252) of QuantSeq 3' mRNA-seq FWD Library Prep Kit (Lexogen). Briefly, 50 ng of extracted RNA was denatured for 30 s at 85 °C with oligo(dT) primers containing an Illumina-compatible sequence at its 5' end followed by reverse transcription at 42 °C for 1 h. After RNA removal, the second strand of cDNA was synthesized by a random primer containing an Illumina-compatible linker sequence at its 5' end. Finally, individual sample barcodes (dual indexing) for multiplexing were introduced via 15 cycles of PCR (determined by qPCR). All libraries were analyzed for adapter dimers, size distribution, and concentration on a Fragment Analyzer System using the DNF-474 HS NGS Fragment kit (1–6,000 bp) (Agilent). After pooling the libraries in an equimolar ratio, the concentration and the size distribution of the lane mix was analyzed by Qubit dsDNA HS assay (Thermo Fisher Scientific) and by 2100 Bioanalyzer device using the HS-DNA assay (Agilent), respectively. A 2 nM dilution of the lane mix was then denatured and diluted for sequencing. Finally, sequencing of 75 bp reads was performed on an Illumina NextSeq 500 sequencer with a v2 75 cycle High Output kit (Illumina).

Bioinformatic analysis and differential expression analysis

The sample data was demultiplexed from the raw sequencing data using the sample and barcode multiplexing scheme with the software bcl2fastq (v2.20.0.422). Adapter trimming was performed by using the software Cutadapt [93] (https://cutadapt.readthedocs.io/en/stable/). The overall quality of the sequencing method was quantified then with the FastQC tool (https://www.bioinformatics.babraham.ac.uk/projects/fastqc/). The alignments were done in two steps. First with BWA-MEM (http://bio-bwa.sourceforge.net/bwa.shtml) using the reference of *D. sapinea CMW 190* (GenBank assembly accession: GCA_000671355.1). This alignment resulted in a fraction of the input reads aligning to this reference. Second, the remaining reads of this alignment were then used as input for another round of alignments against the target reference transcriptomes *P. nigra* [63] and *P. sylvestris* [64]. For both species, two different alignment

methods (BWA-MEM and Salmon) and single quantification method (Salmon) ([94]; https://combine-lab.github.io/salmon/) was used. BWA-MEM is a widely used short-read aligner that uses the Burrows-Wheeler transform, offering a favorable memory and runtime trade-off [95] Salmon, meanwhile, is a transcriptome quantifier that directly quantifies gene and transcript abundance from RNA-Seq data using a quasi-mapping approach. This approach has been shown to offer high sensitivity and specificity [68]. Alignments with BWA-MEM were sorted with samtools and transformed into binary format ([96]; http://www.htslib.org/).

The differential expression analysis between inoculated and mock samples for each provenance was done with DESeq2 package [97], which is implemented in the Bioconductor platform [98, 99] in R [100]. The null hypothesis tested, inclusive of both provenances, implied that the logarithmic fold change in gene expression between infected and mock plants was exactly zero. Significant DEGs were assessed using standard parameters of DESeq2 and adjusted (FDR) p-value < 0.1. This threshold was selected because our results focused on the overlapping set of genes (RELAXED) from the different alignments, making this choice appropriate. PCA was used to visualize sample-to-sample variance, and the input for this analysis was normalized using read counts obtained with the rlog transformation of DESeq2. Finally, Venn diagrams of up- and down-regulated transcripts were created by using jvenn [101].

Annotation of reference transcriptomes and gene ontology enrichment analysis

Even though annotations for both the *P. nigra* and *P. sylvestris* reference transcriptomes were available from the literature, for better comparison, the transcriptomes were annotated using the Taxonomy-oriented Annotation (TOA) pipeline [102] in the amino acid annotation mode. TOA is a transcriptome annotation platform with a focus on plants. Information from genomic databases was used sequentially in this order: Gymno PLAZA 1.0, Dicots PLAZA 4.0, Monocots PLAZA 4.0, NCBI RefSeq Plant and NCBI Nucleotide Database (NT, selecting plant sequences), complemented with information from NCBI Gene, InterPro, and Gene Ontology databases was implemented in the pipeline. Based on this annotation, a further 2,365 transcripts were removed from the published *P. nigra* transcriptome as contaminants (updated accession ERZ9534504). This *P. nigra* transcriptome contained 97,990 transcripts, of which 32,157 got annotated, 24,871 with a GO-term. The *P. sylvestris* transcriptome contained 1.3 million transcripts, of which 166,493 got annotated, of which 123,503 received a GO-term. The lower number of annotated transcripts here, compared to the 236,906 transcripts with a GO-term in the annotation published together with the reference transcriptome, is due to differences in the annotation method as we only annotated detected ORFs.

Gene sets associated with biological processes (BP), molecular functions (MF), and cellular components (CC) were tested for GO terms enrichment using the R-package *topGO* [103]. As input for the analysis, we selected those differentially expressed genes that were detected in both Austrian and Corsican provenances with at least one of the mapping approaches (BWA-MEM and Salmon) for each reference species (*P. nigra* or *P. sylvestris*). The default "weight01" algorithm associated with a Fisher's exact test was applied to select the most relevant terms [103, 104]. A p-value < 0.05 was applied for the statistical test, and no FDR was calculated because the p-values returned by the "weight01" method were interpreted by [103] as corrected or not affected by multiple testing.

KEGG annotation

Homology is a fruitful tool for mapping conserved (orthologous) genes and therewith we analyzed changes in well described and characterized pathways and genes. Metabolic pathway and orthology-oriented functional annotations of the transcript sequences (.fasta files) were performed against the Kyoto Encyclopedia of Genes and Genomes (KEGG) database [105] using the KEGG Automatic Annotation Server (KAAS; https://www.genome.jp/tools/kaas/) [106]. KEGG Orthology (KO) assignment was applied using the Bi-directional Best Hit (BBH) method and all datasets of dicot plants, monocot plants and a basal magnoliophyte were selected as reference organisms (Table S9). This analysis was applied for all differentially up- and down-regulated genes. *P.nigra* pathway hierarchy model was created by merging all plant reference pathway hierarchies available at KEGG (Table S10) and was used to standardize the KO assignment results (Table S3-S4).

Orange Data Mining (https://orange.biolab.si); [107] was used to plot heat maps as a graphical method for visualizing up-/down-regulated pathways and genes among samples. Samples and pathways/genes were sorted by clustering for similarity. In this analysis, k-means was used for grouping, and hierarchical clustering with average linkage was applied for clustering rows. Here, Euclidean distance was used as distance metric.

Identification and quantification of plant hormones

Material (100 mg fresh weight) was suspended in 80% methanol – 1% acetic acid containing internal standards and the extract was shaken for one hour at 4°C. The extract was kept at –20°C overnight and then centrifuged, and the supernatant was then dried in a vacuum evaporator. The dry residue was dissolved in 1% acetic acid and passed through an Oasis HLB reverse phase

column as described in [108] and [109]. For gibberellic acids (Gas), indole-3-acetic acid (IAA), abscisic acid (ABA), salicylic acid (SA) and jasmonic acid (JA) quantification, the dried eluate was dissolved in water 5% acetonitrile—1% acetic acid, and the hormones were separated using an autosampler and reverse phase UHPLC chromatography (2.6 µm Accucore RP-MS column, 100 mm length × 2.1 mm i.d.; Thermo Fisher Scientific) with a 5 to 50% acetonitrile gradient containing 0.05% acetic acid at 400 µL/min over 21 min.

For cytokinins (CKs), the extracts were additionally passed through an Oasis MCX (cationic exchange) and eluted with 60% methanol—5% NH_4OH to obtain the basic fraction containing cytokinins. The final eluate was dried and dissolved in 5% acetonitrile—1% acetic acid and cytokinins were separated with a 5 to 50% acetonitrile gradient over 10 min.

The hormones were analyzed with a Q-Exactive mass spectrometer (Orbitrap detector; Thermo Fisher Scientific) using targeted Selected Ion Monitoring (SIM). The concentrations of hormones in the extracts were determined using embedded calibration curves and the Xcalibur 4.0 and TraceFinder 4.1 SP1 programs. The embedded calibration curve is obtained by representing the Area C/Area C* ratio as a function of different concentrations of C (ppb), for a given concentration of C* (ppb) (1 ppb in case of D-GAs or D-CKs, and 50 ppb in case of D-IAA, D-JA, D-ABA and D-SA). The value of the quotient Ccurva/C*curve, is the value obtained in the curve from the area ratio of the extract (Area C/Area C *) obtained with Q-Exactive, and C*curve is the constant value used to construct the curve. The method for quantification is based in an embedded calibration curve to measure the concentration of each of the analytes based on its direct relationship with the concentration of the added deuterated form.

The internal standards for quantification of each of the different plant hormones were deuterium-labelled hormones, except for JA, for which the compound dihydrojasmonic acid (dhJA) was used. Unpaired t-test was used to assess statistical differences. The internal standards for quantification of GA1, GA4, ABA, IAA, SA, DHZ, iP, tZ, and JA plant hormones are listed in Table S11. Concentration of the internal standards used for hormone profiling was 50 ppb for ABA, IAA, SA and JA, and for active gibberellins GA1, GA4 and cytokinins DHZ, iP, and tZ was 1 ppb.

Identification and quantification of phenolic compounds and diterpenes

From all time points, 50 mg of frozen ground tissue were resuspended in 500 µL of 75% acetonitrile with 1 ppm genistein as the internal standard. The homogenate was vortexed, sonicated for 10 min, and centrifuged for 5 min at 14,000 rpm. Supernatants were filtered with a 0.2 µM filter. Four biological replicates per time point were extracted and analyzed.

The LC-HRMS analysis was performed on an Orbitrap Exploris 120 mass spectrometer coupled with a Vanquish UHPLC System (Thermo Fisher Scientific). LC was carried out by reverse-phase ultraperformance liquid chromatography using a Acquity PREMIER BEH C18 UPLC column (1.7 µM particle size, dimensions 2.1 × 150 mm) (Waters Corp, Mildford, MA, USA).

During sample running, the mobile phase consisted of 0.1% formic acid in water (phase A), and 0.1% formic acid in acetonitrile (phase B). The solvent gradient program was conditioned as follows: 0.5% solvent B over the first 2 min, 0.5—30% solvent B over 25 min, 30—100% solvent B over 13 min, 2 min at 100% B, return to the initial 0.5% solvent B over 1 min, and conditioning at 0.5% B for 2 min. The flow rate was 0.4 ml/min and the injection volume was 1 µL. The column temperature was set at 40ºC.

Ionization was performed with heated electrospray ionization (H-ESI) in positive and negative mode. Samples were acquired in full scan mode (resolution set at 120,000 measured at FWHM) and mixes were acquired in both full scan and data dependent acquisition (DDA) to help with compound identification. For DDA, resolution was set at 30,000 and the intensity threshold at 2e5. Mass range *m/z* was 150 to 1500.

Peak identification and annotation, data analysis, and statistics were performed with Compound Discoverer 3.3 software (Thermo Fisher Scientific). PCA analysis and hierarchical clustering was performed with Metaboanalyst 6.0 [110]. After logarithmic transformation, data scaling was performed by mean centering and dividing by the standard deviation of each variable. Clustering was performed using Euclidean distance measure and the Ward clustering method.

To obtain a general view on how the infection affected the phenolic profiles in both provenances, an untargeted LC–MS metabolic profiling was performed. For a first clean-up of the raw data, only peaks with assigned formula containing C, H and O and with at least one match in database searches were kept and subjected to statistical analysis. After ANOVA and t-test analyses, 889 features with log2FC > 1 and adjusted p-value < 0.05 (Benjamini–Hochberg correction) for at least one comparison were kept. This feature list was subjected to more stringent conditions (log2FC > 2, adjusted p-value < 0.01) and manually curated. For manual curation, features not compatible with molecular formula containing only C, H and O elements were removed (specific search for phenolics and terpenoids). Features distant less than 0.01 min were grouped and treated as corresponding to the same compound. Compound identification included

adducts analysis to retrieve a final molecular formula and selection of the compound name according to criteria specified in supplementary Table S6: authentic standard, compatible retention time, MS/MS data available, correspondence with spectral libraries or previous identification of the compound in the bibliography.

Identification and quantification of VOCs

Pine needles were frozen in liquid nitrogen and powdered. 100 mg samples of frozen powder were resuspended in 1 mL of a saturated NaCl solution, sonicated for 5 min, and subjected to headspace solid phase microextraction (HS-SPME) using a 65 µM Polydimethylsiloxane/Divinylbenzene (PDMS/DVB) fiber (Supelco, Bellefonte, PA, USA). Pre-incubation and extraction were performed at 50ºC for 10 and 20 min, respectively. Desorption was performed for 1 min at 250ºC in a split 1:3 mode. VOCs trapped in the fiber were analyzed by GC–MS using a 6890 N gas chromatograph (Agilent) coupled with a 5975B Inert XL MSD mass spectrometer (Agilent). The column used was an Agilent J&W Scientific DB-5 fused silica capillary column (5%—phenyl—95%—dimethylpolysiloxane as the stationary phase, 60 m length, 0.25 mm i.d., and 1 mm thickness film). Oven temperature conditions were 40ºC for 2 min, 5ºC min^{-1} ramp until 250ºC and then held isothermally at 250ºC for 5 min. Helium was used as carrier gas at 1.4 ml min^{-1} constant flow. M/z detection was obtained by an Agilent mass spectrometer operating in the EI mode (ionization energy, 70 eV; source temperature 230ºC). Data acquisition was performed in scanning mode (mass range m/z 35–220). Chromatograms and spectra were recorded and processed using Masshunter software (Agilent). Compound identification was based on both the comparison between the MS for each putative compound with those of the NIST Mass Spectral library and the match to our retention time and Mass Spectra custom library generated using commercially available compounds. Data analysis and visualization was performed using Simca-P software (Umetrics, Sweden) and MetaboAnalyst [110].

Abbreviations

ABA	Abscisic acid
BBH	Bi-directional Best Hit
BP	Biological process (GO category)
CC	Cellular component (GO category)
CKs	Cytokinins
DDA	Data dependent acquisition
DEGs	Differentially expressed genes
DHZ	Dihydrozeatin
dpi	Days post-inoculation
ETI	Effector-triggered immunity
GO	Gene ontology
GAs	Gibberellins
HS-SPME	Headspace solid phase microextraction
IAA	Indole-3-acetic acid (indole acetic acid)
JA	Jasmonic acid
KAAS	KEGG Automatic Annotation Server
KEGG	Kyoto Encyclopedia of Genes and Genomes
KO	KEGG Orthology
MAPK	Mitogen-activated protein kinase
MPK6	Mitogen-activated protein kinase 6
PCA	Principal component analysis
PR1	Pathogenesis-related protein 1
PTI	Pattern-triggered immunity
RGs	Reference genes
RIN	RNA integrity numbers
SA	Salicylic acid
SE	Standard error
SEM	Standard error of the mean
SIM	Selected Ion Monitoring
SIR	Systemic induced resistance
SIS	Systemic induced susceptibility
TIC	Total ion current
TOA	Taxonomy-oriented Annotation
tZ	Trans-zeatin
VOCs	Volatile organic compounds

Supplementary Information

The online version contains supplementary material available at https://doi.org/10.1186/s12864-026-12582-5.

Supplementary Material 1.

Acknowledgements

The authors express their gratitude for the financial support for the creation of the analyzed data provided by the Austrian federal government and provinces and the European Union (project Askforgen, grant number LE 14-20/8.5.2-III4-01/18). They would like to offer special thanks to Fernando Mora-Márquez and Unai López de Heredia for their valuable assistance in setting up the TOA pipeline on a local computer, and to Tanja Pyhäjärvi for providing annotation information on the P. sylvestris transcriptome. Recognition is given to technicians Michaela Breuer and Teresa Caballero Vizcaíno for sample processing and technical advice, as well as Michael Kober-Eberhardt and Dominik Lorenschitz for their contributions to the experiment performance. The authors also acknowledge the Supercomputing Centre of Galicia (CESGA) and CSC – Finnish IT Center for the allocation of computational resources. They also express sincere appreciation to Agathe Hurel and Saúl Ares for critical reading of the manuscript. Finally, the authors would like to thank Lila Afifi for her review of the last version and her efforts to improve the grammar and organization of the paper.

Authors' contributions

J-PG, EH, CTM and MvL conceived the project concept. CTM, MvL, SM-K and EH planned and coordinated the experiment; MvL and SM-K performed the experiment and conducted sampling. SM-K prepared the inoculum and cultivated the ***Diplodia sapinea***. OG and BV contributed to the selection of ***P. sylvestris*** ortholog candidate defense-related genes. CTM designed the primers for the candidate defense-related genes and RE performed the RNA isolation and RT-qPCR analyses. SO led the scientific advice for the cDNA sequencing (mRNA-seq) and mapping to the available reference transcriptomes with different alignment methods, performed annotation of reference transcriptomes and gene ontology enrichment analysis. CTM performed the KEGG annotation. MA and CP prepared samples for the metabolomic analyses. EC and JB performed the identification and quantification of plant hormones. AER and MÁM-G performed the identification and quantification of phenolic compounds, diterpenes and VOCs. CTM and SO wrote the manuscript with contributions from all authors. BF and AG provided scientific and editorial advice. All authors reviewed and approved the final version of the manuscript. CTM and SO contributed equally and are both first authors.

Funding

Austrian federal government and provinces and the European Union (project Askforgen, grant number LE 14–20/8.5.2-III4-01/18).

Data availability
Raw sequence data have been submitted to the NCBI Short Read Archive (SRA) under BioProject number PRJNA1122172. The updated ***P. nigra*** transcriptome was uploaded to EMBL (accession HBZE01000000 under BioProject PRJEB33411). The metabolomics data have been deposited to MetaboLights [111] repository with the study identifier MTBLS13184 and MTBLS13216.

Declarations

Ethics approval and consent to participate
Not applicable.

Consent for publication
Not applicable.

Competing interests
The authors declare no competing interests.

Author details
[1]Austrian Research Centre for Forests (BFW) - Department of Forest Growth, Silviculture & Forest Genetics, Seckendorff-Gudent-Weg 8, Vienna 1131, Austria
[2]Institute of Forest Sciences, (ICIFOR-INIA), Consejo Superior de Investigaciones Científicas (CSIC), Crta. Coruña Km 7.5, Madrid 28040, Spain
[3]BOKU University, Institute of Forest Entomology, Forest Pathology and Forest Protection (IFFF), Peter-Jordan-Straße 82/I, Vienna 1190, Austria
[4]University of Veterinary Medicine, VetCore Facility for Research, Veterinärplatz 1, Vienna 1210, Austria
[5]Georg-August-University of Göttingen, Forest Genetics and Forest Tree Breeding, Büsgenweg 2, Göttingen 37077, Germany
[6]National Research Institute for Agriculture, Food and Environment - Ecology of Mediterranean Forests (INRAE-URFM), Domaine St Paul, Avignon 84914, France
[7]Department of Botany, University of Innsbruck, Sternwartestraße 15, Innsbruck 6020, Austria
[8]Institute for Plant Molecular and Cell Biology (IBMCP), Consejo Superior de Investigaciones Científicas (CSIC) - Universidad Politécnica de Valencia (UPV), Calle Ingeniero Fausto Elio, S/N, Valencia 46022, Spain
[9]Terrestrial Ecosystem Research, Centre for Microbiology and Environmental System Science, University of Vienna, Djerassiplatz 1, Vienna 1030, Austria
[10]Natural Resources Institute Finland (LUKE), Latokartanonkaari 9, Helsinki 00790, Finland

Received: 25 April 2025 / Accepted: 19 January 2026
Published online: 30 January 2026

References

1. Allen CD, Macalady AK, Chenchouni H, Bachelet D, McDowell N, Vennetier M, et al. A global overview of drought and heat-induced tree mortality reveals emerging climate change risks for forests. For Ecol Manage. 2010;259:660–84. https://doi.org/10.1016/j.foreco.2009.09.001.
2. Desprez-Loustau ML, Marçais B, Nageleisen LM, Piou D, Vannini A. Interactive effects of drought and pathogens in forest trees. Ann For Sci. 2006;63:597–612. https://doi.org/10.1051/forest:2006040.
3. Seidl R, Thom D, Kautz M, Martin-Benito D, Peltoniemi M, Vacchiano G, et al. Forest disturbances under climate change. Nat Clim Chang. 2017;7:395–402. https://doi.org/10.1038/nclimate3303.
4. Hanewinkel M, Cullmann DA, Schelhaas MJ, Nabuurs GJ, Zimmermann NE. Climate change may cause severe loss in the economic value of European forest land. Nat Clim Chang. 2013;3:203–7. https://doi.org/10.1038/nclimate1687.
5. Enescu CM, de Rigo D, Caudullo G, Houston Durrant T. Pinus nigra in Europe: distribution, habitat, usage and threats. In: European Atlas of Forest Tree Species. 2016. pp. 126-7.
6. Trujillo-Moya C, Ganthaler A, Stöggl W, Arc E, Kranner I, Schueler S, et al. Advances in understanding Norway spruce natural resistance to needle bladder rust infection: transcriptional and secondary metabolites profiling. BMC Genomics. 2022;23:435. https://doi.org/10.1186/s12864-022-08661-y.
7. Hammerbacher A, Raguschke B, Wright LP, Gershenzon J. Gallocatechin biosynthesis via a flavonoid 3′,5′-hydroxylase is a defense response in Norway spruce against infection by the bark beetle-associated sap-staining fungus *Endoconidiophora polonica*. Phytochemistry. 2018;148:78–86. https://doi.org/10.1016/j.phytochem.2018.01.017.
8. Liu JJ, Sturrock RN, Benton R. Transcriptome analysis of Pinus monticola primary needles by RNA-seq provides novel insight into host resistance to Cronartium ribicola. BMC Genomics. 2013;14. https://doi.org/10.1186/1471-2164-14-884.
9. Hernandez-Escribano L, Visser EA, Iturritxa E, Raposo R, Naidoo S. The transcriptome of Pinus pinaster under Fusarium circinatum challenge. BMC Genomics. 2020;21. https://doi.org/10.1186/s12864-019-6444-0.
10. Weiss M, Sniezko RA, Puiu D, Crepeau MW, Stevens K, Salzberg SL, et al. Genomic basis of white pine blister rust quantitative disease resistance and its relationship with qualitative resistance. Plant J. 2020;104:365–76. https://doi.org/10.1111/tpj.14928.
11. Ganthaler A, Stöggl W, Mayr S, Kranner I, Schüler S, Wischnitzki E, et al. Association genetics of phenolic needle compounds in Norway spruce with variable susceptibility to needle bladder rust. Plant Mol Biol. 2017;94. https://doi.org/10.1007/s11103-017-0589-5.
12. Vallauri DR, Aronson J, Barbero M. An analysis of forest restoration 120 years after reforestation on Badlands in the Southwestern Alps. Restor Ecol. 2002;10:16–26. https://doi.org/10.1046/j.1526-100X.2002.10102.x.
13. Isajev V, Fady B, Semerci H, Andonovski V. EUFORGEN [European Forest Genetic Resources Programme] technical guidelines for genetic conservation and use for European black pine (Pinus nigra). EUFORGEN Technical Guidelines for Genetic Conservation and Use. 2004.
14. Saladin B, Leslie AB, Wüest RO, Litsios G, Conti E, Salamin N, et al. Fossils matter: improved estimates of divergence times in Pinus reveal older diversification. BMC Evol Biol. 2017;17. https://doi.org/10.1186/s12862-017-0941-z.
15. Scotti-Saintagne C, Giovannelli G, Scotti I, Roig A, Spanu I, Vendramin GG, et al. Recent, Late Pleistocene fragmentation shaped the phylogeographic structure of the European black pine (Pinus nigra Arnold). Tree Genet Genomes. 2019;15. https://doi.org/10.1007/s11295-019-1381-2.
16. Thiel D, Nagy L, Beierkuhnlein C, Huber G, Jentsch A, Konnert M, et al. Uniform drought and warming responses in Pinus nigra provenances despite specific overall performances. For Ecol Manage. 2012;270. https://doi.org/10.1016/j.foreco.2012.01.034.
17. Vacek Z, Cukor J, Vacek S, Gallo J, Bažant V, Zeidler A. Role of black pine (Pinus nigra J. F. Arnold) in European forests modified by climate change. European Journal of Forest Research. 2023;142. https://doi.org/10.1007/s10342-023-01605-5.
18. Stanosz GR, Smith DR, Guthmiller MA. Characterization of Sphaeropsis sapinea from the West Central United States by means of random amplified polymorphic DNA marker analysis. Plant Dis. 1996;80. https://doi.org/10.1094/PD-80-1175.
19. de Wet J, Wingfield MJ, Coutinho TA, Wingfield BD. Characterization of Sphaeropsis sapinea isolates from South Africa, Mexico, and Indonesia. Plant Dis. 2000;84. https://doi.org/10.1094/PDIS.2000.84.2.151.
20. Slippers B, Wingfield MJ. Botryosphaeriaceae as endophytes and latent pathogens of woody plants: diversity, ecology and impact. Fungal Biol Rev. 2007;21:90–106. https://doi.org/10.1016/j.fbr.2007.06.002.
21. Bihon W, Slippers B, Burgess T, Wingfield MJ, Wingfield BD. Sources of Diplodia pinea endophytic infections in Pinus patula and P. radiata seedlings in South Africa. For Pathol. 2011;41:370–5. https://doi.org/10.1111/j.1439-0329.2010.00691.x.
22. Thorpe K. Diseases of trees and shrubs. Forestry. 2006;79:612–3. https://doi.org/10.1093/forestry/cpl039.
23. Decourcelle T, Piou D, Desprez-Loustau ML. Detection of Diplodia sapinea in Corsican pine seeds. Plant Pathol. 2015;64:442–9. https://doi.org/10.1111/ppa.12263.
24. Luchi N, Oliveira Longa CM, Danti R, Capretti P, Maresi G. *Diplodia sapinea* : the main fungal species involved in the colonization of pine shoots in Italy. For Pathol. 2014;44:372–81. https://doi.org/10.1111/efp.12109.
25. PIOU D, CHANDELIER P, MORELET M. Sphaeropsis sapinea, un nouveau problème sanitaire des Pins en France ? Revue Forestière Française. 1991; 203. https://doi.org/10.4267/2042/26199.
26. Flowers J, Nuckles E, Hartman J, Vaillancourt L. Latent infection of Austrian and Scots pine tissues by Sphaeropsis sapinea. Plant Dis. 2001;85. https://doi.org/10.1094/PDIS.2001.85.10.1107.

27. Stanosz GR, Blodgett JT, Smith DR, Kruger EL. Water stress and *Sphaeropsis sapinea* as a latent pathogen of red pine seedlings. New Phytol. 2001;149:531–8. https://doi.org/10.1046/j.1469-8137.2001.00052.x.
28. Blumenstein K, Bußkamp J, Langer GJ, Langer EJ, Terhonen E. The *Diplodia* tip blight pathogen *Sphaeropsis sapinea* is the most common fungus in Scots pines' mycobiome, irrespective of health status—a case study from Germany. J Fungi. 2021;7:607. https://doi.org/10.3390/jof7080607.
29. Hurel A, de Miguel M, Dutech C, Desprez-Loustau ML, Plomion C, Rodríguez-Quilón I, et al. Genetic basis of growth, spring phenology, and susceptibility to biotic stressors in maritime pine. Evol Appl. 2021;14:2750–72. https://doi.org/10.1111/eva.13309.
30. Bußkamp J, Langer GJ, Langer EJ. *Sphaeropsis sapinea* and fungal endophyte diversity in twigs of Scots pine (*Pinus sylvestris*) in Germany. Mycol Progress. 2020;19(9):985–99. https://doi.org/10.1007/s11557-020-01617-0.
31. Brodde L, Adamson K, Julio Camarero J, Castaño C, Drenkhan R, Lehtijärvi A, et al. Diplodia Tip Blight on Its Way to the North: Drivers of Disease Emergence in Northern Europe. Front Plant Sci. 2019;9. https://doi.org/10.3389/fpls.2018.01818.
32. Smith DR, Stanosz GR. A species-specific PCR assay for detection of *Diplodia pinea* and *D. scrobiculata* in dead red and jack pines with collar rot symptoms. Plant Dis. 2006;90:307–13. https://doi.org/10.1094/PD-90-0307.
33. Luchi N, Pratesi N, Simi L, Pazzagli M, Capretti P, Scala A, et al. High-resolution melting analysis: a new molecular approach for the early detection of *Diplodia pinea* in Austrian pine. Fungal Biol. 2011;115:715–23. https://doi.org/10.1016/j.funbio.2011.05.005.
34. Luchi N, Capretti P, Surico G, Orlando C, Pazzagli M, Pinzani P. A real-time quantitative PCR assay for the detection of *Sphaeropsis sapinea* from inoculated *Pinus nigra* shoots. J Phytopathol. 2005;153:37–42. https://doi.org/10.1111/j.1439-0434.2004.00924.x.
35. Aday Kaya AG, Yeltekin Ş, Lehtijärvi TD, Lehtijärvi A, Woodward S. Severity of diplodia shoot blight (caused by diplodia sapinea) was greatest on pinus sylvestris and pinus nigra in a plantation containing five pine species. Phytopathol Mediterr. 2019;58:249–59. https://doi.org/10.14601/Phytopathol_Mediter-10613.
36. Koltay A. Susceptibility of different clone groups of Austrian pine to Mycosphaerella pini E. Rostrup and Sphaeropsis sapinea Dyko & Sutton. Acta Silvatica Lignaria Hungarica. 2007;Special:47-51.
37. Hu B, Mithöfer A, Reichelt M, Eggert K, Peters FS, Ma M, et al. Systemic reprogramming of phytohormone profiles and metabolic traits by virulent Diplodia infection in its pine (*Pinus sylvestris* L.) host. Plant Cell Environ. 2021;44:2744–64. https://doi.org/10.1111/pce.14061.
38. Bonello P, Gordon TR, Herms DA, Wood DL, Erbilgin N. Nature and ecological implications of pathogen-induced systemic resistance in conifers: A novel hypothesis. Physiol Mol Plant Pathol. 2006;68. https://doi.org/10.1016/j.pmpp.2006.12.002.
39. Eyles A, Chorbadjian R, Wallis C, Hansen R, Cipollini D, Herms D, et al. Cross-induction of systemic induced resistance between an insect and a fungal pathogen in Austrian pine over a fertility gradient. Oecologia. 2007;153:365–74. https://doi.org/10.1007/s00442-007-0741-z.
40. Eyles A, Bonello P, Ganley R, Mohammed C. Induced resistance to pests and pathogens in trees. New Phytol. 2010;185:893–908. https://doi.org/10.1111/j.1469-8137.2009.03127.x.
41. Blodgett JT, Eyles A, Bonello P. Organ-dependent induction of systemic resistance and systemic susceptibility in *Pinus nigra* inoculated with *Sphaeropsis sapinea* and *Diplodia scrobiculata*. Tree Physiol. 2007;27:511–7. https://doi.org/10.1093/treephys/27.4.511.
42. Sherwood P, Bonello P. Testing the systemic induced resistance hypothesis with Austrian pine and *Diplodia sapinea*. Physiol Mol Plant Pathol. 2016;94:118–25. https://doi.org/10.1016/j.pmpp.2016.06.002.
43. Sherwood P, Villari C, Capretti P, Bonello P. Mechanisms of induced susceptibility to *Diplodia* tip blight in drought-stressed Austrian pine. Tree Physiol. 2015;35(5):549–62. https://doi.org/10.1093/treephys/tpv026.
44. Ghosh SK, Slot JC, Visser EA, Naidoo S, Sovic MG, Conrad AO, et al. Mechanisms of Pine Disease Susceptibility Under Experimental Climate Change. Front Forests Glob Change. 2022;5 June:1-21. https://doi.org/10.3389/ffgc.2022.872584.
45. Hu B, Sakakibara H, Kojima M, Takebayashi Y, Bußkamp J, Langer GJ, et al. Consequences of Sphaeropsis tip blight disease for the phytohormone profile and antioxidative metabolism of its pine host. Plant Cell Environ. 2018;41. https://doi.org/10.1111/pce.13118.
46. Hu B, Liu Z, Haensch R, Mithöfer A, Peters FS, Vornam B, et al. Diplodia sapinea infection reprograms foliar traits of its pine (Pinus sylvestris L.) host to death. Tree Physiol. 2023;43. https://doi.org/10.1093/treephys/tpac137.
47. Wallis C, Eyles A, Chorbadjian RA, Riedl K, Schwartz S, Hansen R, et al. Differential effects of nutrient availability on the secondary metabolism of Austrian pine (*Pinus nigra*) phloem and resistance to *Diplodia pinea*. For Pathol. 2011;41:52–8. https://doi.org/10.1111/j.1439-0329.2009.00636.x.
48. Bonello P, Blodgett JT. *Pinus nigra-Sphaeropsis sapinea* as a model pathosystem to investigate local and systemic effects of fungal infection of pines. Physiol Mol Plant Pathol. 2003;63:249–61. https://doi.org/10.1016/j.pmpp.2004.02.002.
49. Wallis C, Eyles A, Chorbadjian R, McSpadden Gardener B, Hansen R, Cipollini D, et al. Systemic induction of phloem secondary metabolism and its relationship to resistance to a canker pathogen in Austrian pine. New Phytol. 2008;177:767–78. https://doi.org/10.1111/j.1469-8137.2007.02307.x.
50. Sherwood P, Bonello P. Austrian pine phenolics are likely contributors to systemic induced resistance against *Diplodia pinea*. Tree Physiol. 2013;33:845–54. https://doi.org/10.1093/treephys/tpt063.
51. Ganthaler A, Guggenberger A, Stöggl W, Kranner I, Mayr S. Elevated nutrient supply can exert worse effects on Norway spruce than drought, viewed through chemical defence against needle rust. Tree Physiol. 2023;43. https://doi.org/10.1093/treephys/tpad084.
52. Ghosh SK, Ishangulyyeva G, Erbilgin N, Bonello P. Terpenoids are involved in the expression of systemic-induced resistance in Austrian pine. Plant Cell Environ. 2024;47. https://doi.org/10.1111/pce.14875.
53. Bonello P, Capretti P, Luchi N, Martini V, Michelozzi M. Systemic effects of *Heterobasidion annosum* s.s. infection on severity of *Diplodia pinea* tip blight and terpenoid metabolism in Italian stone pine (*Pinus pinea*). Tree Physiol. 2008;28:1653–60. https://doi.org/10.1093/treephys/28.11.1653.
54. Gershenzon J, Dudareva N. The function of terpene natural products in the natural world. Nat Chem Biol. 2007;3:408–14. https://doi.org/10.1038/nchembio.2007.5.
55. Hall DE, Yuen MMS, Jancsik S, Quesada AL, Dullat HK, Li M, et al. Transcriptome resources and functional characterization of monoterpene synthases for two host species of the mountain pine beetle, lodgepole pine (Pinus contorta) and jack pine (Pinus banksiana). BMC Plant Biol. 2013;13. https://doi.org/10.1186/1471-2229-13-80.
56. Carrasco A, Wegrzyn JL, Durán R, Fernández M, Donoso A, Rodriguez V, et al. Expression profiling in *Pinus radiata* infected with *Fusarium circinatum*. Tree Genet Genomes. 2017;13:46. https://doi.org/10.1007/s11295-017-1125-0.
57. Trujillo-Moya C, Ganthaler A, Stöggl W, Kranner I, Schüler S, Ertl R, et al. RNA-Seq and secondary metabolite analyses reveal a putative defence-transcriptome in Norway spruce (Picea abies) against needle bladder rust (Chrysomyxa rhododendri) infection. BMC Genomics. 2020;21. https://doi.org/10.1186/s12864-020-6587-z.
58. Ding X, Diao S, Luan Q, Wu HX, Zhang Y, Jiang J. A transcriptome-based association study of growth, wood quality, and oleoresin traits in a slash pine breeding population. PLoS Genet. 2022;18. https://doi.org/10.1371/journal.pgen.1010017.
59. Neale DB, Wegrzyn JL, Stevens KA, Zimin A V., Puiu D, Crepeau MW, et al. Decoding the massive genome of loblolly pine using haploid DNA and novel assembly strategies. Genome Biol. 2014;15. https://doi.org/10.1186/gb-2014-15-3-r59.
60. Fox H, Doron-Faigenboim A, Kelly G, Bourstein R, Attia Z, Zhou J, et al. Transcriptome analysis of *Pinus halepensis* under drought stress and during recovery. Tree Physiol. 2018;38:423–41. https://doi.org/10.1093/treephys/tpx137.
61. Gaspar D, Trindade C, Usié A, Meireles B, Barbosa P, Fortes AM, et al. Expression profiling in Pinus pinaster in response to infection with the pine wood nematode Bursaphelenchus xylophilus. Forests. 2017;8. https://doi.org/10.3390/f8080279.
62. Vornam B, Leinemann L, Peters FS, Wolff A, Leha A, Salinas G, et al. Response of Scots pine (*Pinus sylvestris*) seedlings subjected to artificial infection with the fungus *Sphaeropsis sapinea*. Plant Mol Biol Rep. 2019;37:214–23. https://doi.org/10.1007/s11105-019-01149-2.
63. Olsson S, Grivet D, Cattonaro F, Vendramin V, Giovannelli G, Scotti-Saintagne C, et al. Evolutionary relevance of lineages in the European black pine (*Pinus nigra*) in the transcriptomic era. Tree Genet Genomes. 2020;16:30. https://doi.org/10.1007/s11295-020-1424-8.
64. Ojeda DI, Mattila TM, Ruttink T, Kujala ST, Kärkkäinen K, Verta JP, et al. Utilization of tissue ploidy level variation in de novo transcriptome assembly of

Pinus sylvestris. G3 Genes|Genomes|Genetics. 2019;9:3409–21. https://doi.org/10.1534/g3.119.400357.
65. Metsämuuronen S, Sirén H. Bioactive phenolic compounds, metabolism and properties: a review on valuable chemical compounds in Scots pine and Norway spruce. Phytochem Rev. 2019;18:623–64. https://doi.org/10.1007/s11101-019-09630-2.
66. Mukrimin M, Kovalchuk A, Ghimire RP, Kivimäenpää M, Sun H, Holopainen JK, et al. Evaluation of potential genetic and chemical markers for Scots pine tolerance against Heterobasidion annosum infection. Planta. 2019;250. https://doi.org/10.1007/s00425-019-03270-8.
67. Sahlin K. Strobealign: flexible seed size enables ultra-fast and accurate read alignment. Genome Biol. 2022;23. https://doi.org/10.1186/s13059-022-02831-7.
68. Srivastava A, Malik L, Sarkar H, Zakeri M, Almodaresi F, Soneson C, et al. Alignment and mapping methodology influence transcript abundance estimation. Genome Biol. 2020;21. https://doi.org/10.1186/s13059-020-02151-8.
69. Blumenstein K, Bußkamp J, Langer GJ, Langer EJ, Terhonen E. The diplodia tip blight pathogen sphaeropsis sapinea is the most common fungus in scots pines' mycobiome, irrespective of health status—a case study from germany. J Fungi. 2021;7. https://doi.org/10.3390/jof7080607.
70. Webster C, Figueroa-Corona L, Méndez-González ID, Álvarez-Soto L, Neale DB, Jaramillo-Correa JP, et al. Comparative analysis of differential gene expression indicates divergence in ontogenetic strategies of leaves in two conifer genera. Ecol Evol. 2022;12. https://doi.org/10.1002/ece3.8611.
71. Han Z, Xiong D, Schneiter R, Tian C. The function of plant PR1 and other members of the CAP protein superfamily in plant–pathogen interactions. Mol Plant Pathol. 2023;24. https://doi.org/10.1111/mpp.13320.
72. Breen S, Williams SJ, Outram M, Kobe B, Solomon PS. Emerging Insights into the Functions of Pathogenesis-Related Protein 1. Trends Plant Sci. 2017;22. https://doi.org/10.1016/j.tplants.2017.06.013.
73. Meng X, Xu J, He Y, Yang KY, Mordorski B, Liu Y, et al. Phosphorylation of an ERF transcription factor by Arabidopsis MPK3/MPK6 regulates plant defense gene induction and fungal resistance. Plant Cell. 2013;25. https://doi.org/10.1105/tpc.112.109074.
74. Bigeard J, Hirt H. Nuclear signaling of plant MAPKs. Front Plant Sci. 2018;9. https://doi.org/10.3389/fpls.2018.00469.
75. Pandey D, Rajendran SRCK, Gaur M, Sajeesh PK, Kumar A. Plant defense signaling and responses against necrotrophic fungal pathogens. J Plant Growth Regul. 2016;35. https://doi.org/10.1007/s00344-016-9600-7.
76. Jagodzik P, Tajdel-Zielinska M, Ciesla A, Marczak M, Ludwikow A. Mitogen-activated protein kinase cascades in plant hormone signaling. Front Plant Sci. 2018;9. https://doi.org/10.3389/fpls.2018.01387.
77. Kazan K, Manners JM. MYC2: The master in action. Mol Plant. 2013;6. https://doi.org/10.1093/mp/sss128.
78. Du M, Zhao J, Tzeng DTW, Liu Y, Deng L, Yang T, et al. MYC2 orchestrates a hierarchical transcriptional cascade that regulates jasmonate-mediated plant immunity in tomato. Plant Cell. 2017;29. https://doi.org/10.1105/tpc.16.00953.
79. Veluthakkal R, Sundari BKR, Dasgupta MG. Tree chitinases – stress- and developmental-driven gene regulation. For Pathol. 2012;42:271–8. https://doi.org/10.1111/j.1439-0329.2011.00759.x.
80. Uzma Jalil S, Mishra M, Ansari MI. Current view on chitinase for plant defence. 2015.
81. Kumar M, Brar A, Yadav M, Chawade A, Vivekanand V, Pareek N. Chitinases—potential candidates for enhanced plant resistance towards fungal pathogens. Agriculture (Basel). 2018;8:88. https://doi.org/10.3390/agriculture8070088.
82. Nickolov K, Gauthier A, Hashimoto K, Laitinen T, Väisänen E, Paasela T, et al. Regulation of PaRBOH1-mediated ROS production in Norway spruce by Ca2+ binding and phosphorylation. Front Plant Sci. 2022;13. https://doi.org/10.3389/fpls.2022.978586.
83. Chong J, Poutaraud A, Hugueney P. Metabolism and roles of stilbenes in plants. Plant Sci. 2009;177. https://doi.org/10.1016/j.plantsci.2009.05.012.
84. Rafii ZA, Dodd RS, Zavarin E. Genetic diversity in foliar terpenoids among natural populations of European black pine. Biochem Syst Ecol. 1996;24. https://doi.org/10.1016/0305-1978(96)00028-2.
85. Fkiri S, Mezni F, Rigane G, Ben Salem R, Ghazghazi H, Khouja ML, et al. Chemotaxonomic Study of Four Subspecies of Pinus nigra Arn. Grown in Common Garden Based on Essential Oil Composition. J Food Qual. 2021;2021. https://doi.org/10.1155/2021/5533531.
86. Niu S, Li J, Bo W, Yang W, Zuccolo A, Giacomello S, et al. The Chinese pine genome and methylome unveil key features of conifer evolution. Cell. 2022;185. https://doi.org/10.1016/j.cell.2021.12.006.
87. Blodgett JT, Bonello P. The aggressiveness of Sphaeropsis sapinea on Austrian pine varies with isolate group and site of infection. For Pathol. 2003;33. https://doi.org/10.1046/j.1439-0329.2003.00303.x.
88. Zwolinski JB, Swart WJ, Wingfield MJ. Intensity of dieback induced by Sphaeropsis sapinea in relation to site conditions. Eur J Forest Pathol. 1990;20. https://doi.org/10.1111/j.1439-0329.1990.tb01127.x.
89. Stanosz GR, Trobaugh J, Guthmiller MA, Stanosz JC. Sphaeropsis shoot blight and altered nutrition in red pine plantations treated with paper mill waste sludge. For Pathol. 2004;34. https://doi.org/10.1111/j.1439-0329.2004.00366.x.
90. Altschul SF, Gish W, Miller W, Myers EW, Lipman DJ. Basic local alignment search tool. J Mol Biol. 1990;215. https://doi.org/10.1016/S0022-2836(05)80360-2.
91. Xie F, Xiao P, Chen D, Xu L, Zhang B. miRDeepFinder: A miRNA analysis tool for deep sequencing of plant small RNAs. Plant Mol Biol. 2012;80. https://doi.org/10.1007/s11103-012-9885-2.
92. Livak KJ, Schmittgen TD. Analysis of relative gene expression data using real-time quantitative PCR and the 2-ΔΔCT method. Methods. 2001;25. https://doi.org/10.1006/meth.2001.1262.
93. Martin M. Cutadapt removes adapter sequences from high-throughput sequencing reads. EMBnet J. 2011;17. https://doi.org/10.14806/ej.17.1.200.
94. Patro R, Duggal G, Love MI, Irizarry RA, Kingsford C. Salmon provides fast and bias-aware quantification of transcript expression. Nat Methods. 2017;14. https://doi.org/10.1038/nmeth.4197.
95. Burrows M, Wheeler D. A block-sorting lossless data compression algorithm. Algorithm, Data Compression. 1994. https://www.cs.jhu.edu/~langmea/resources/burrows_wheeler.pdf}
96. Li H, Handsaker B, Wysoker A, Fennell T, Ruan J, Homer N, et al. The Sequence Alignment/Map format and SAMtools. Bioinformatics. 2009;25. https://doi.org/10.1093/bioinformatics/btp352.
97. Love MI, Huber W, Anders S. Moderated estimation of fold change and dispersion for RNA-seq data with DESeq2. Genome Biol. 2014;15. https://doi.org/10.1186/s13059-014-0550-8.
98. Gentleman RC, Carey VJ, Bates DM, Bolstad B, Dettling M, Dudoit S, et al. Bioconductor: open software development for computational biology and bioinformatics. Genome Biol. 2004;5. https://doi.org/10.1186/gb-2004-5-10-r80}
99. Huber W, Carey VJ, Gentleman R, Anders S, Carlson M, Carvalho BS, et al. Orchestrating high-throughput genomic analysis with Bioconductor. Nat Methods. 2015;12. https://doi.org/10.1038/nmeth.3252.
100. R Core Team. R: A language and environment for statistical computing. R Foundation for Statistical Computing, Vienna, Austria. Open J Stat. 2023;13. https://www.R-project.org/}
101. Bardou P, Mariette J, Escudié F, Djemiel C, Klopp C. Jvenn: An interactive Venn diagram viewer. BMC Bioinformatics. 2014;15. https://doi.org/10.1186/1471-2105-15-293.
102. Mora-Márquez F, Chano V, Vázquez-Poletti JL, López de Heredia U. TOA: A software package for automated functional annotation in non-model plant species. Mol Ecol Resour. 2021;21:621-36. https://doi.org/10.1111/1755-0998.13285.
103. Alexa A, Rahnenführer J. Gene topGO: Enrichment Analysis for Gene Ontology enrichment analysis with topGO. R package version 2.48.0. Bioconductor Improvments. 2022. https://bioconductor.statistik.tu-dortmund.de/packages/3.15/bioc/vignettes/topGO/inst/doc/topGO.pdf}
104. Alexa A, Rahnenfuhrer J, Lengauer T. Improved scoring of functional groups from gene expression data by decorrelating GO graph structure. Bioinformatics. 2006;22:1600–7. https://doi.org/10.1093/bioinformatics/btl140.
105. Kanehisa M, Furumichi M, Tanabe M, Sato Y, Morishima K. KEGG: New perspectives on genomes, pathways, diseases and drugs. Nucleic Acids Res. 2017;45. https://doi.org/10.1093/nar/gkw1092.
106. Moriya Y, Itoh M, Okuda S, Yoshizawa AC, Kanehisa M. KAAS: An automatic genome annotation and pathway reconstruction server. Nucleic Acids Res. 2007;35 SUPPL.2. https://doi.org/10.1093/nar/gkm321.
107. Demšar J, Curk T, Erjavec A, Gorup Č, Hočevar T, Milutinovič M, et al. Orange: Data mining toolbox in python. J Machine Learn Res. 2013;14. http://jmlr.org/papers/v14/demsar13a.html}
108. Seo M, Jikumaru Y, Kamiya Y. Profiling of hormones and related metabolites in seed dormancy and germination studies. Methods Mol Biol. 2011;773. https://doi.org/10.1007/978-1-61779-231-1_7.

109. Binenbaum J, Wulff N, Camut L, Kiradjiev K, Anfang M, Tal I, et al. Gibberellin and abscisic acid transporters facilitate endodermal suberin formation in Arabidopsis. Nat Plants. 2023;9. https://doi.org/10.1038/s41477-023-01391-3.
110. Pang Z, Lu Y, Zhou G, Hui F, Xu L, Viau C, et al. MetaboAnalyst 6.0: towards a unified platform for metabolomics data processing, analysis and interpretation. Nucleic Acids Res. 2024;1-9. https://doi.org/10.1093/nar/gkae253.
111. Yurekten O, Payne T, Tejera N, Amaladoss FX, Martin C, Williams M, et al. MetaboLights: open data repository for metabolomics. Nucleic Acids Res. 2024;52. https://doi.org/10.1093/nar/gkad1045.

Publisher's Note